ČESKÁ ZEMĚDĚLSKÁ UNIVERZITA V PRAZE

TECHNICKÁ FAKULTA

APLIKACE FOTOVOLTAICKÝCH ČLÁNKŮ A PANELŮ

Katedra fyziky

Disertáční Práce

Práci vypracoval: **Ing. MINH QUAN DANG**

Školitel disertační práce: **doc. Ing. Vladislav Poulek, CSc.**

V Praze 2019

CZECH UNIVERSITY OF LIFE SCIENCES PRAGUE

FACULTY OF ENGINEERING

APPLICATION

OF

PHOTOVOLTAIC SOLAR CELLS AND PANELS

Department of Physics

Dissertation

PhD Student: **Ing. MINH QUAN DANG**

Doctoral thesis supervisors: **doc. Ing. Vladislav Poulek, CSc.**

Prague 2019

PROHLÁŠENÍ

Prohlašuji, že jsme tuto disertační práci vypracoval samostatně pod vedením školitele a uvedl jsem veškerou použitou literaturu. Tištěná a elektronická verze práce se doslovně shodují

JMÉNO A PŘÍJMENÍ:

PODPIS:

DATUM:

PODĚKOVÁNÍ

Nejprve bych chtěl poděkovat mému školiteli doc. Ing. Vladislavu Poulkovi, CSc. za odborné vedení a konzultace v průběhu studia doktorského studijního programu, za přínosné rady a připomínky k disertační práci.

Také chci poděkovat prof. Ing. Martinu Librovi, CSc. za konzultace k metodologickému zpracování práce a podporu při studiu, Mgr. Bohumilu Chalupovi a Ing. Pavelu Kouřímovi za praktické rady a doporučení.

V neposlední řadě patří mé poděkování mojí rodině za emoční a materiální podporu při studiu.

ABSTRAKT

Tato práce zkoumá inovativní konstrukci fotovoltaických panelů s integrovanými bateriemi (FV-baterie - panel) pro použití v ostrovním režimu. Prototyp tohoto panelu byl zkonstruován na katedře fyziky a poté instalován na terasu budovy Technické fakulty za účelem vyhodnocení jeho parametrů. Výsledek testů prokázal, že prototyp je během provozu bezpečný. Tato práce také zkoumá FV-baterie - panel z hlediska ekonomické analýzy. Simulace ukazuje, že jeden PV-baterie - panel by mohl zajistit poměr energetické soběstačnosti větší než 90% pouze u systémů, které vyžadují roční spotřebu nižší než 0,1 MWh za rok. Provoz systému je silně ovlivněn špičkovým zatížením a rozložením zatížení. FV systém s FV-bateriemi – panely je efektivní, když je spotřeba energie větší než 0,5 MWh za rok s dobou návratnosti 10 let a NPV je 1,806 Kč. Větší FV systém může být konstruován s více moduly pracujími paralelně.

Kličová slova: FV systém, Skladování energie, Off-grid systém, modul FV-baterie, Proveditelnost

ABSTRACT

This work is exploring the innovative concept of a photovoltaic-battery integration module (PV-battery module) for off-grid application. A prototype of this concept has been made on the physics department and then installed on the roof of 2nd floor, block 3, faculty of Engineering building to evaluate its physical properties. The result from tests and long-term observation proof that prototype is safe during its operation. This work is also investigating the feasibility of a PV-battery module prototype through techno-economic analysis. Simulation show that one PV-battery module could ensure a self-sufficiency ratio greater than 90% only for systems requiring an annual consumption less than 0.1 MWh per year. The system operation is strongly affected by the peak load demand and load profile. Single PV-battery module becomes feasible when energy demand is larger than 0.5 MWh per year with 10 years payback period and NPV is CZK 1,806. Larger system could be reached with more modules operate in parallel.

Key words: PV system, Energy Storage, Off-grid system, PV-battery module , Feasibility

TABLE OF CONTENTS

LIST OF FIGURES

LIST OF TABLES

LIST OF ABBREVIATIONS

PV	Photovoltaic
a-Si	Amorphous silicon
BMS	Battery management system
BSS	Battery storage system
CdTe	Cadmium telluride
CIGS	Copper-indium-gallium-diselenide
CIS	Copper indium selenide
c-Si	Crystalline silicon
CULS	Czech university of life sciences in Prague
HIJ	Heterojunction
IBC	Interdigitated back contact
LCO	Lithium cobalt oxide
LFP	Lithium iron phosphate
LMO	Lithium manganese oxide
LTO	Lithium titanate
MWT	Metal-wrap-through
NCA	Lithium nickel cobalt aluminum oxide
NMC	Lithium nickel manganese cobalt oxide
NPV	Net Present Value
P/E ratio	Power to energy ratio
PERC	Passivated emitter and a rear cell
SOC	State of charge
SOH	State of health

INTRODUCTION

Energy is essential for human activities. We need fuel for traveling, electric energy for lighting, thermal energy for heating, and many others. This work focuses on only the path of electric energy, and more specifically that from photovoltaic (PV) power. Mankind is facing today an increasing energy demand around the world year after year, and conventional energy resources such as fossil fuels cannot be used forever because of their limited volumes and because the climate suffers from global warming. On the other hand, innovation in solar PV technology and battery technology allow manufacturers to produce solar PV cell and battery with higher power and capacity for less price.

The first chapter presents general facts on the photovoltaic system such as current status, physic, and technology. Within this chapter, the author briefly describes the energy storage with lithium-ion battery and application from another effort to build an integrated PV-battery module.

Chapter two presents the hypothesis and objectives of the work.

Chapter three presents the research method which was used within this work. In this chapter issues and difficulties during the designing process and its solution is described. Structure of the PV-battery and installation set up is also provided. A techno-economical model is proposed for further study of this concept.

Chapter four provides results from safety evaluation tests of the PV-battery module and long-term temperature observation of the module. In these tests, the module design is proven to be safe.

In chapter five, a series of analysis using the techno-economical model are made to study the feasibility of the PV-battery module under various situations. The results identify appropriate situation when the user could use the module.

The final chapter is the general work conclusion follow with author contribution and suggestion for future work.

Chapter 1. OVERVIEW OF PROBLEM STATUS

1.1 BACKGROUND

Energy is essential for human activities. We need fuel for traveling, electric energy for lighting, thermal energy for heating, and many others. This work focuses on only the path of electric energy, and more specifically that from photovoltaic (PV) power. The world's primary energy consumption in 2016 was 13,276.3 MTOE. Most energy used today is derived from the sun. The majority, approximately 85.5%, of the world's primary energy consumption in 2016 was converted from fossil fuels, even though the share has decreased during the last decades (British Petroleum, 2017).

Energy demand around the world is increasing year after year, especially in Asian countries. To meet the increasing demand, new energy resources must be exploited. Conventional energy resources such as fossil fuels cannot be used forever because of their limited volumes and because the climate suffers from global warming (GUIFANG, et al., 2017). For these reasons, renewable energy will most likely play a vital role in the transformation of the energy system. One main challenge to solve is how to store renewable energy. It is often possible to store biomass and hydropower for use when energy demand is high, but wind, wave, and solar power are more difficult to store. A PV system with storage is the main subject of this work.

The installed capacity for PV power has increased rapidly in recent years. In 2016, approximately 2.1% of the global electricity demand was covered by PV electricity production (British Petroleum, 2017). Europe dominated the market for several years at the beginning of the 21st century, mainly due to subsidies for renewable energy resources. The market for PV installation is now mainly driven by Asian countries, with China (53 GW) and USA (10.6 GW) ranked 1 and 2 in 2017, followed by India (9.1 GW). In 2017, there were 29 countries with more than 1 GW of cumulative PV system capacity (MASSON, et al., 2018). PV solar energy must take a much bigger part in total energy consumption of the world before the mid-21st century to confront climate change and avoid environmental disaster.

1.2 PHOTOVOLTAIC PHYSIC, SOLAR CELLS, AND STATE-OF-THE-ART TECHNOLOGIES

Visible sunlight is only a small part of the total energy emitted by the sun to the earth's surface. The famous works of Planck and Einstein described the light as the flow of indistinguishable energy elements called photons (PLANCK, 1901) (EINSTEIN, 1905). A photon may appear as either a wave or as a particle depending on the situation. This concept is called "wave-particle duality."

$$E = \frac{hc}{\lambda} \tag{1.1}$$

Where

E is the energy of the photon in eV with wavelength λ [μm];

h is Planck's constant = 6.626×10^{-34} joule s;

c is the speed of light = 2.998×10^{8} m/s

The characteristics of incident solar radiation on the earth's surface could be categorized by the spectral content of the incident light, the radiant power density from the sun, the angle at which the incident solar radiation strikes an interesting surface, and the radiant energy throughout a period of time (Honsberg, et al., 2019). The amount of solar energy reaching the surface of the Earth every hour is greater than the amount of energy used by the Earth's population over an entire year (HARRINGTON, 2017). The radiation on the Earth surface varies because of local effects such as clouds and seasonal climate as well as location and latitude.

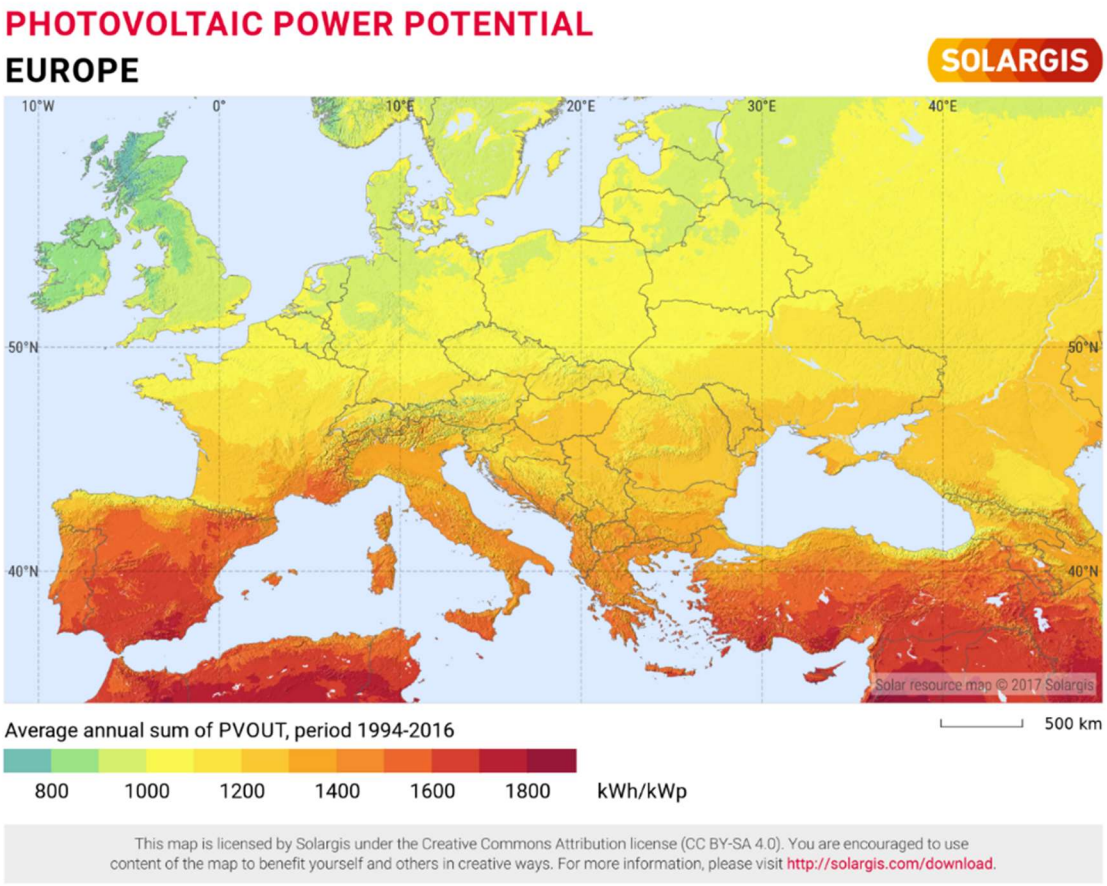

Figure 1. Solar irradiation in Europe

An important part of the physics of photovoltaic phenomenon is the band gap (POULEK, et al., 2010). The band gap defines the energy required for an incoming photon to be able to excite an electron in the material. A conducting material such as a metal has no or very low band gap; a semiconductor has a moderate band gap, and an insulator the highest band gap. Solar cells are semiconductors, and the moderate band gap is both low enough to be able to absorb photons and excite electrons and high enough to generate a potential difference. The vast majority of the solar cells produced today have only one layer (one band gap), which sets a limit of the efficiency of conversion of solar irradiance into electricity,

known as the Shockley–Queisser limit (SHOCKLEY, et al., 1961). Single-band-gap solar cells have a maximum theoretical efficiency close to 40% with a normal solar spectrum according to the Shockley–Queisser limit, whereas other calculations show a limit around 30% (PETERS, et al., 2018). However, the highest theoretical efficiency depends on whether or not the light is concentrated. Two or more layers with different band gaps are needed to further enhance the efficiency of solar cells; these are called tandem cells (two layers) and multi-layer cells (YAMAGUCHI, et al., 2018) (LIU, et al., 2018) (GUIFANG, et al., 2017).

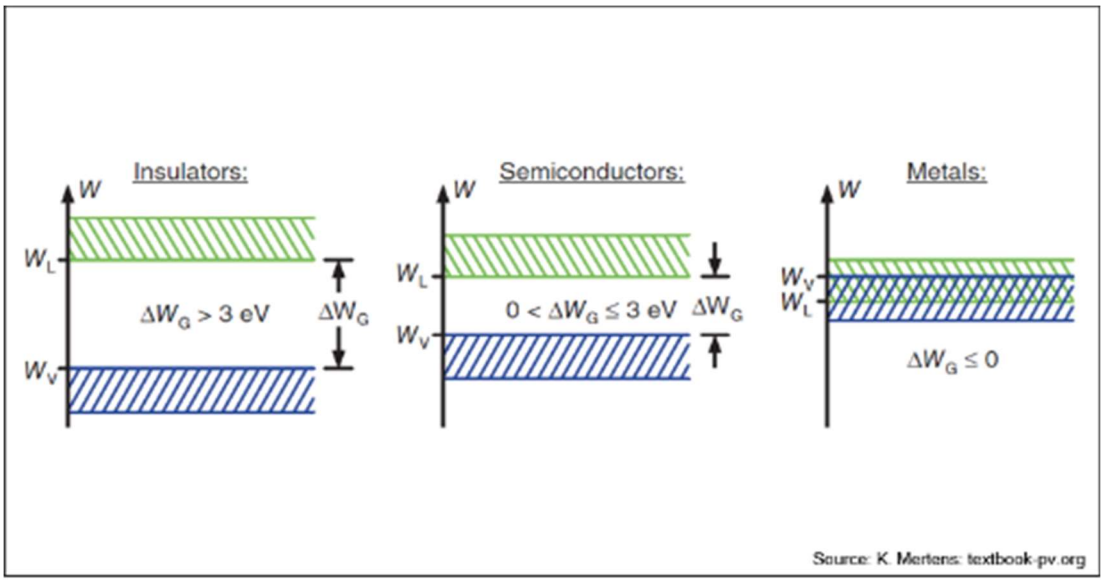

Figure 2. Band gap of different materials (MERTENS, 2014)

The solar cell is the basic building block of the PV system consisting of semiconductor materials. The semiconductors behave like conductors when exposed to light or heat, but at low temperature the semiconductor becomes insulators. Normally, the semiconductor material consists of at least two layers. Positive charge (holes) located on one

layer (p-type), and negative charge on the other layer (n-type). When the cell is exposed to light, the atoms of the semiconductor absorb some photons from the light and release an electron from the cell's negative layer. The external circuit allows the flow of the released electron back to the positive layer, which represents the electric current.

Solar cells use the energy in incoming photons from the sun to excite electrons to a higher energy state in the material. Normally, the excited electrons return quickly to the initial energy state without contributing to any useful energy output. In PV cells, however, a built-in asymmetry prevents the electrons from returning to their initial energy state, and a potential difference, i.e., voltage, between the two sides of the solar cells is generated. Each cell has a voltage of 0.5–1 V when illuminated. A PV module with a higher voltage can be obtained by connecting several PV cells in series (POULEK, et al., 2010).

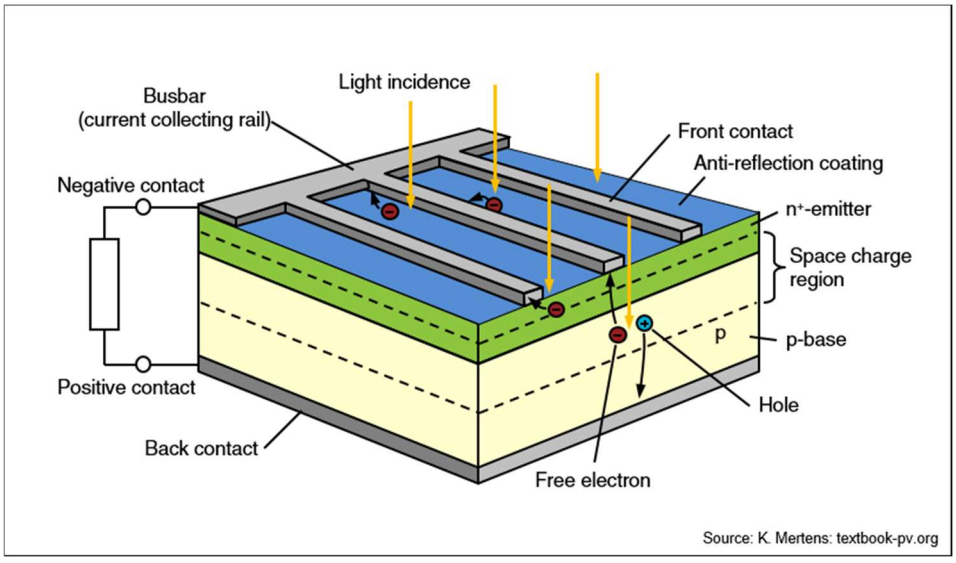

Figure 3. Structure of solar cell (MERTENS, 2014)

The physical construction of a solar cell is shown in Figure 3. In general, a solar cell consists of top contacts, single or double layers of anti-reflective coating, an n-type emitter, a p-type base, and a back contact (MERTENS, 2014). The purpose of the top contacts is to collect current from the emitter and to connect the solar cell to an external circuit. An anti-reflection coating is applied to minimize light reflection from the solar cell. The anti-reflection coating maximizes the light entering the cell, which increases the solar cell output power (CHEN, 2001). An n-type emitter and p-type base are the main components of the solar cell. The emitter layer, which contains the negative majority electrons, is made as thin as possible to attain reasonable sheet resistivity. Practically, the emitter layer thickness is approximately 2 μm. On the other side, the base layer is thicker than the emitter layer, as it is almost the full thickness of the solar cell. Typically, the thickness of a silicon solar cell is about 200–500 μm. The rear contact is located at the bottom of the solar cell. It is mainly used to collect the charge carriers and to reflect the light back into the optical path (WÜRFEL, et al., 2009)

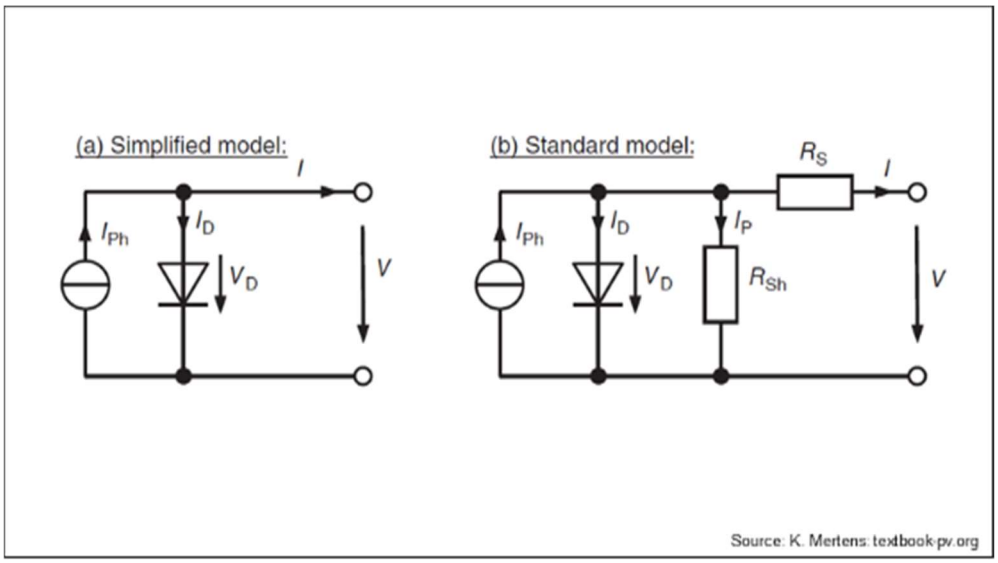

Figure 4. Equivalent circuit of a solar cell (MERTENS, 2014)

The equivalent circuit of the solar cell consists of a photocurrent source, a diode, a parallel resistor to model the leakage current, and a series resistor to describe the internal resistance. The equivalent circuit of a solar cell is shown in Figure 4. The physical model of the generated current in a PV system using the equivalent circuit of the solar cell is represented by the following equation (MERTENS, 2014):

$$I = I_{\mathrm{Ph}} - I_{\mathrm{S}}\left(e^{\frac{V+IR_{\mathrm{S}}}{mV_{\mathrm{T}}}} - 1\right) - \frac{V + IR_{\mathrm{S}}}{R_{\mathrm{Sh}}} \qquad (1.2)$$

Where

V and I represent the PV array output voltage and current, respectively.

R_s and R_{sh} are the solar cell series and shunt resistances;

I_{Ph} is the light generated current;

I_S is the saturation current;

m is the ideality factor (usually between 1 and 2)

V_T is thermal voltage

A PV module (PV module) consists of a group of solar cells that are series-connected to obtain enough working voltage. Usually, the PV module is rated by its dc output power under standard test conditions (STC) and commercially STC is specified at an irradiance of 1,000 W/m^2 with a spectral distribution of air mass (AM) 1.5 and a 25℃ PV cell temperature (WOHLGEMUTH, 2012).

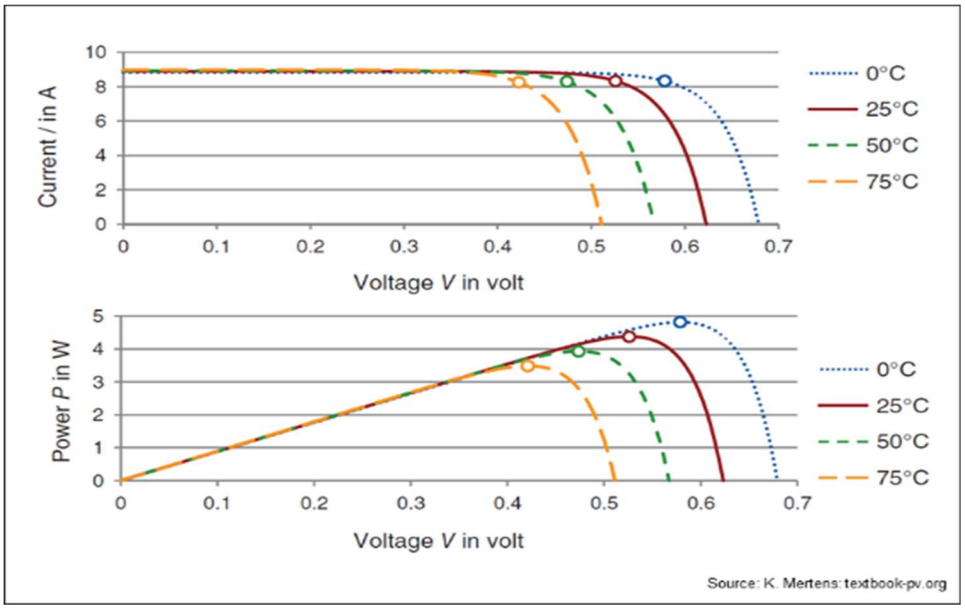

Figure 5. I–V and P–V characteristics of the solar cell (MERTENS, 2014)

1.3 GENERATIONS OF PV TECHNOLOGY

1.3.1 First-generation PV technology

The first generation of PV modules uses the wager-based crystalline silicon (c-Si) technology, either monocrystalline or multicrystalline silicon. The crystalline module first appeared in 1963 when Sharp Corporation started mass producing it and installed the first commercial PV power system on a lighted buoy in Japan (GREEN, 2001). Following Sharp's success, different technologies for silicon-based PV modules have been introduced over the last five decades.

PERC: Passivated emitter and a rear cell has a passivation layer in the back of the PV cell. This layer is able to reflect the long wavelength sunlight back to the cell to increase the efficiency and decrease rear current carrier losses by reducing the rear-side recombination. PERC monocrystalline cells can reach an efficiency of 23.6% and at the module level can reach 20.41% efficiency (HALL, 2019).

MWT: Metal-wrap-through technology allows both positive and negative electrodes distributed on the rear side of solar cells to reduce the busbar shading problem. This cell structure allows the PV module to have lower power degradation and lower operating temperature (GUILLEVIN, et al., 2012).

Black Silicon: Nanotexturing technology can be used to create an inverted pyramid diamond-like structure on the surface of the PV cell to capture the light inside the cell. This technology could reduce the energy yield to 3% and thus reduce energy cost (BLACK, et al., 2017).

Half-cell: The cells are cut in half, and the electrical circuit is connected for each half of the PV module separately. This reduces the electrical current flowing on the busbar by half, and resistive losses of the PV module are reduced, resulting in an increase of power by 3% (QCELLS, 2018).

HIJ: A heterojunction structure using a thin intrinsic amorphous silicon layer between the c-Si wafer and doped layer reduces recombination losses and increases cell efficiency (ROTERS, et al., 2010).

IBC: Interdigitated back contact solar cells eliminate shading losses by putting both contacts on the rear cell. This design allows the PV cell to be put closer to each other because the interconnection could be printed on the back side, such as an electronic board (YOSHIKAWA, et al., 2017).

1.3.2 Second-generation PV technology

The second generation of PV modules is based on thin-film PV technologies and includes three main families: amorphous (a-Si), cadmium telluride (CdTe), copper indium selenide (CIS), and copper-indium-gallium-diselenide (CIGS).

The first thin-film solar cells were based on amorphous silicon (a-Si). The technology is most commonly used in devices that require very little power (e.g., pocket calculators) because of its low efficiency (13.4%). The amorphous silicon PV module has lost its position on the global market because of its low efficiency.

Cadmium telluride (CdTe) solar cells consist of a simple p–n heterojunction structure containing a p-doped CdTe layer matched with an n-doped cadmium sulfide (CdS) layer, which acts as a window layer. CdTe solar cells are completed by adding a high-quality transparent conductive oxide (TCO)—usually fluorine-doped tin oxide (SnO_2:F)—and a back electrical contact—typically a metal or carbon paste with copper (Cu). First Solar is the main manufacturer producing CdTe thin-film PV modules. It latest product is called First Solar Series 6 and has a module efficiency up to 18% for the 445 Wp module (First-Solar, 2019). However, there are environmental issues with products that rely on cadmium, a heavy metal and potential carcinogen that can accumulate in plant and animal tissue. Although the threat is minimal as long as the compound is contained within the solar module, the disposal and recycling can be both dangerous and costly.

Copper indium diselenide ($CuInSe_2$) thin-film technology has been considered promising for solar cells because of its favorable electronic and optical properties. It was later found that by substituting gallium (Ga) for indium (In), the bandgap can be increased from about 1.04 electron-volts (eV) for copper indium diselenide (CIS) films to about 1.68 eV for copper gallium diselenide (CGS) films. Although laboratory-scale cell efficiencies have exceeded 20%, commercial CIS modules typically have efficiencies between 12 and 14.2% (AVANCIS, 2019).

1.3.3 Third-generation PV technology

Third-generation approaches to photovoltaics (PVs) aim to achieve high-efficiency devices but still use thin-film, second-generation deposition methods. The main approaches for this generation are multi-junction cells, intermediate-band cells, hot carrier cells, and spectrum conversion. Multi-junction cells use multiple solar cells that selectively absorb different regions of the solar spectrum. Intermediate-band cells use one junction with multiple bandgaps to increase efficiencies. Hot-carrier cells convert the excess energy of above-bandgap photons into electrical energy. Spectrum conversion solar cells convert the incoming polychromatic sunlight into a narrower distribution of photons suited to the bandgap of the solar cell (BROWN, et al., 2009).

1.4 LITHIUM BATTERY AS ENERGY-STORAGE SYSTEM

Lithium-ion (Li-ion) batteries are well-known power components of portable electronic devices such as smartphones, tablets, and laptops. In combination with the electricity grid, Li-ion batteries could support the integration of high shares of photovoltaic (PV) and wind energy in the power mix by providing storage capacity and ancillary services.

The first lithium battery was built in the 1970s by Michael Stanley Whittingham, who used lithium metal and titanium sulfide as electrodes (WHITTINGHAM, 1976). The four main components of a Li-ion battery cell are the cathode, anode, electrolyte, and separator. During charge, the lithium ions move from the cathode, through the electrolyte, to the anode, and move back during discharge. Current commercial batteries are named for the lithium-ion donor in the cathode, as this is the main determinant of cell properties. Several lithium metal oxides are used for this purpose: lithium cobalt oxide (LCO), lithium manganese oxide (LMO), lithium iron phosphate (LFP), lithium nickel cobalt aluminum oxide (NCA), and lithium nickel manganese cobalt oxide (NMC). This variety of materials results in significantly different battery characteristics (NITTA, et al., 2015). The current dominant anode material is graphite, although some battery manufacturers have opted for non-graphite anodes such as lithium titanate (LTO, $Li_4Ti_5O_{12}$) (MOORTHI, 2010). The electrolyte is a mixture of a lithium salt and organic solvents. Common lithium salts include lithium-hexafluorophosphate (LiPF6), lithium perchlorate ($LiClO_4$) and lithium-hexafluoroarsenate ($LiAsF_6$) (ZUBI, et al., 2018). The separator is a safety component between the cathode and

the anode, preventing direct contact, i.e., short-circuiting, while being permeable to lithium ions. The most common separator materials are polyethylene and polypropylene. Li-ion battery cells are manufactured as cylindrical or stack cells.

Liable and safe-to-use Li-ion cells require a battery management system (BMS) to track and manage key functionality and performance aspects, e.g., voltage, current, state of charge (SOC), state of health (SOH), and temperature, among other aspects.

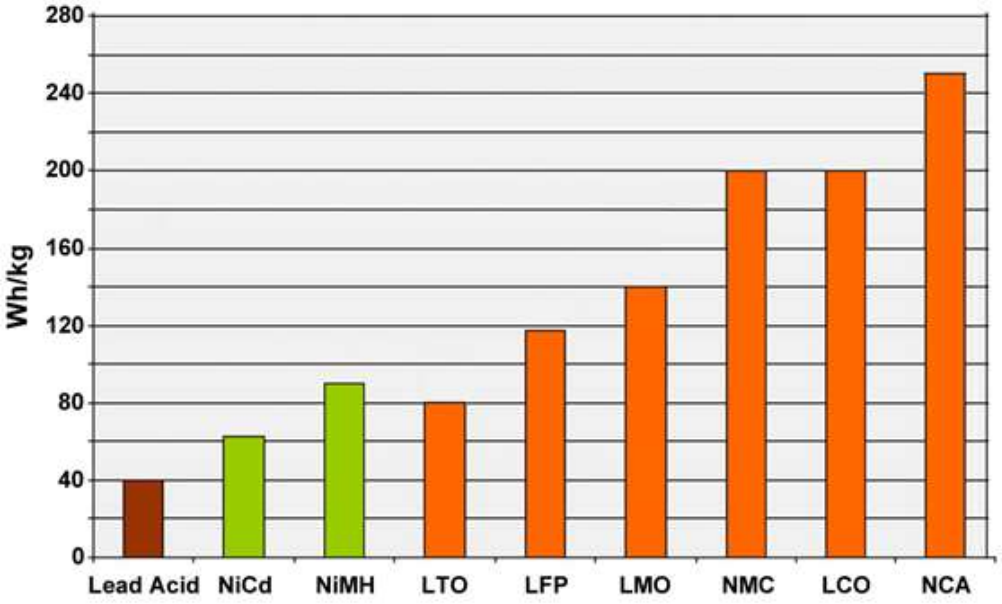

Figure 6. Energy density of different battery technologies (CADEX, 2019)

The most relevant characteristics of a battery are its specific energy and power, durability, and safety. Current commercial Li-ion batteries cover a wide range of specific

energy, roughly from 90 to 250 Wh/kg. NCA batteries perform best in this aspect, whereas LFP batteries perform worse.

The specific power is often described within the power to energy (P/E) ratio, i.e., how much power in kilowatts could a battery provide for a kilowatt-hour of capacity. Another important property of a battery is its durability. Battery degradation occurs in all conditions, but in different proportions depending on the use. Tough operating conditions such as low or high operation temperatures, overcharge, deep discharge, and high amperage accelerate degradation. Batteries suffer calendar and cycle aging; the first occurs even if the battery is stored and therefore depends basically on external conditions, most specifically the temperature. Cycle aging is additionally subject to the battery charge and discharge conditions. A review on the aging mechanisms of Li-ion batteries and the SOH estimation methods is provided in the work of Barré Anthony (BARRÉ, et al., 2013).

Safety issues of Li-ion batteries are extensively investigated, and the challenge is not only how to make current batteries safer in an expanding range of applications but also to improve aspects such as specific energy and power without compromising safety. A serious concern over Li-ion batteries is thermal runaway; if a battery cell is excessively heated, for instance, through prolonged overcharge or short-circuiting, to the level of decomposing its metal oxide, the battery could burst into flame because of the reaction of freed oxygen with lithium. A detailed review of the thermal runaway of Li-ion batteries is provided in (ZHAO, et al., 2018).

Li-ion batteries are still very far from the competitive cost range for grid-connected use. In the short term, a battery bank-specific cost around €300/kWh with a lifetime of around 2,000 cycles is achievable, but this still entails an energy-storage cost greater than €0.20/kWh. Li-ion batteries will be competitive for grid-connected use once specific battery-bank costs are less than €200/kWh with a lifetime above 2,500 cycles. Energy storage in off-grid renewable-energy systems is currently dominated by lead-acid batteries, but in the medium and long terms, Li-ion batteries will emerge as a very competitive technology (JAISWAL, 2017) (DIOUF, et al., 2015). Li-ion batteries have an outstanding advantage over lead-acid in covering the relatively high power requirements. Lithium-ion cells (the basic components of batteries) cost more than $1,000 a kilowatt-hour (kWh) in 2010; in 2017, they were in the $130–200 range (Diego, 2019). Lower costs are not the only improvements; large amounts of R&D investment have led to better power density (more storage per kilogram) and better durability (more discharge-then-recharge cycles).

1.5 PHOTOVOLTAIC-BATTERY INTEGRATION MODULE

System cost is one of the main barriers preventing wide deployment of the PV module. To make it more affordable, the installation can be integrated into one single device to reduce human labor and cost. Effort has been made to integrate the power electronic components directly on the backside of the PV modules by using an inverter or dc–dc converter (WILLS, et al., 1997) (ACANSKI, et al., 2010). Also, the battery was integrated into the module in (REYNAUD, et al., 2008).

The advantages of the integration concept include simplification by reduction of complexity during the design and installation process, flexible output response to the load demand, scalable size by the modular approach, and a portability and ease of deployment in a remote area. However, this kind of system requires PV module with reasonable cost, light weight, high efficiency, and high energy/power density battery with a thermal control method and battery management system. The physical construction of the system also raises a problem, as the system must withstand long-term outdoor operation (VEGA-GARITA, et al., 2016). This work will propose a solution to deal with these challenges.

Chapter 2. SCOPE AND OBJECTIVES

This work contributes to the effort to transform energy sources to cleaner and more sustainable options. The first purpose of this work is exploring the innovative concept of a photovoltaic-battery integration module (PV-battery module) for off-grid application. A prototype of this concept has been made and installed on the physics department to evaluate its physical properties. The second purpose of this work is to investigate the feasibility of a PV-battery module prototype through techno-economic analysis. The analysis was designed to study the PV-battery module use in a single household. The third purpose of this work is to magnify the system for a micro-grid community. This final purpose aims to prepare for a larger deployment of this prototype in a remote area.

Along with the tasks, several hypotheses are set in the beginning of the work as following

- Appropriate set up of solar cells could charge the lithium ion battery without safety issue
- Integration of PV module and battery storage system is feasible for off-grid application.

Chapter 3. RESEARCH METHOD

3.1 OVERVIEW OF RESEARCH METHODS

The first step is conducting literature research for the recent applications of PV cells and modules. This is presented in the literature review above. The research then narrows down to a practical problem for off-grid application.

The small and integrated PV-battery module was designed, and a prototype was created in the Physic Department of CULS. The design has two main tasks, providing effective safety measures to protect the PV-battery module and providing adequate energy supply for a predefined load profile.

For the first task, the problems with the PV-battery module are categorized into mechanical, electrical, and thermal problems. The mechanical problems are solved by using a strong protective profile from aluminum to ensure no external physical contact can be exerted directly on the battery as well as the battery management (BMS) circuit. The internal structure divides the battery bank into four sections to minimize the consequences of a problem if one occurs. Electrical problems are solved by using the battery management system to control the charge and discharge current of the batteries; the battery voltage of each individual cell is monitored. BMS will protect the battery from over/under voltage and overcharging problems.

Furthermore, DC fuses are applied as a secondary protection method. The thermal problem is solved by the passive cooling method. The aluminum cover works as a heat sink to cool the batteries during operation. Multiple thermal sensors are installed on the PV-battery module to record the effectiveness of the cooling system.

The effectiveness of the first task is proved by a series of both long- and short-term tests. The short-term test is a high current discharge of the battery during the day. Those tests try to simulate the worst-case scenario, wherein the system must work during high ambient temperature during the day and supply the high current demand for the load. The tests and result are shown in the next chapter. The effectiveness of the mechanical problem resolution is self-evidence, and further tests will not be conducted because those tests will lead to the destruction of the prototype. The long-term test is via cyclic discharge of the battery during the night and recharge during the day with the PV module. This test tries to simulate the normal condition operation of the off-grid system, wherein most of the load will occur during the night. Dependence of the battery temperature on the ambient temperature was closely monitored with a 3 s interval. The test has run continuously for more than a year to date, and the results are shown in the next chapter.

For the second task, the electrical characteristics of the PV-battery module are measured. Based on that data, a simulation of energy balance is made to examine the feasibility. Details of the techno-economical model are described in section 3.3.

3.2 DESIGN CONCEPT

To combine the PV module with the battery, we faced several obstacles.

Selection of PV technology: We decided to use monocrystalline silicon PV cells in our prototype. This is one of the highest-efficiency PV cells with reasonable cost and easy accessibility.

Selection of PV module so it can provide sufficient energy for battery banks: Because the target of this PV-battery module is for an off-grid system, the battery bank and PV module should have reasonable size and be scalable. The battery banks are designed with a nominal capacity of 1100 Wh, and the PV module is 260 Wp. Under the conditions of Prague, the Czech Republic, the average daily yield is 2.918 kWh/kWp, so the battery could be charged to about 70% every day.

Selection of lithium battery technology: As we discussed above, the safest option is LFP battery, but the NMC has the highest energy density. In the off-grid system, we prioritize energy storage and compensate for the problem with safety by designing a stronger battery holder profile.

Solving the PV-battery module reliability issue during its operation: An aluminum cover profile is made to protect the battery and BMS from external factors as well as isolate the battery in the case of failure.

A glass/glass PV module using polysiloxane encapsulate integrated with 6 Li-ion cells (prismatic) NCM type 40 Ah. The glass/glass structure is stronger and more durable compared to the traditional glass/back sheet structure. The polysiloxane gel encapsulation provides high transparency and extra protection for a solar cell that is extremely suited for off-grid application. The gel has excellent optical properties toward visible and near-infrared spectra. Also, this gel provides outstanding thermal resistance up to +260 ºC, which protects the internal integrity of the module.

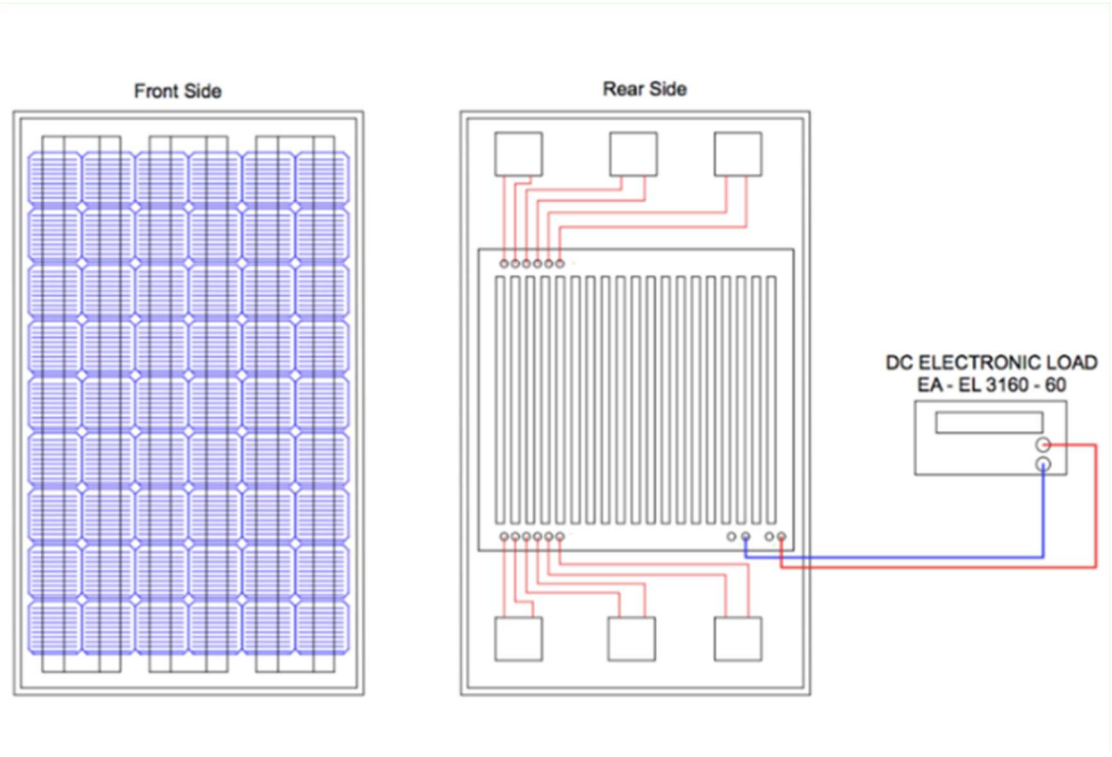

Figure 7. Concept of the front and rear sides of the PV-battery module

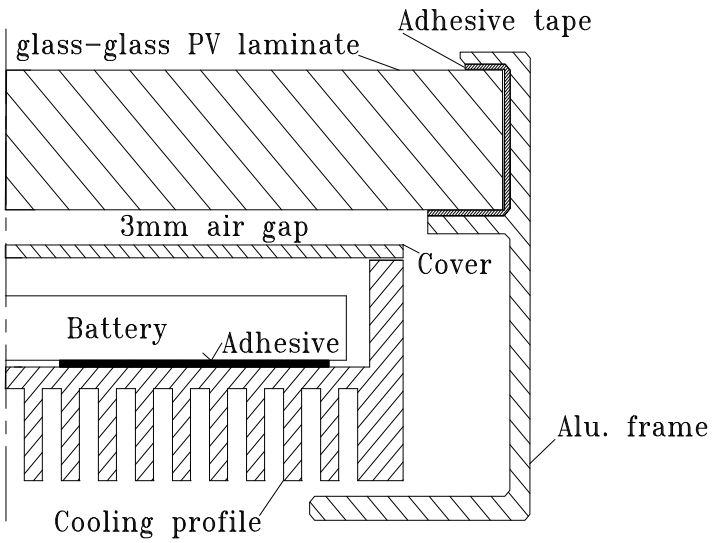

Figure 8. Concept of the cooling profile of the PV-battery module

The PV module was created from 54 mono-crystalline silicon solar cell that provide a power of 260 Wp. The electrical interconnection of the system is shown in Figure 7Figure 9. Table 1 shows the parameters of the PV module used in the prototype. This module is made in the Physics Department of the UCLS technical facility.

Rated power	**260 W**
Tolerance	+/-3%
Efficiency STC	17.5%
V_{mpp}	29.4 V
I_{mpp}	8.8 A
V_{oc}	36.5 V
Temp. coefficient of power (M_{pp})	–0.39%/°C
Voltage coefficient (V_{oc})	–0.31%/°C
Current coefficient	+0.05%/°C
Solar cell layout	9 × 6 (54-cell module)

Table 1. Solar PV module parameters

The array of solar cells connected in series will provide a maximum of ~29.4 V at the battery bank terminals under operating conditions. BMS is used to monitor and protect the battery from under-voltage and over-temperature issues. This feature guarantees the safety from overvoltage problem with the battery. The BMS system is configured as in Table 2. The interconnection inside the aluminum profile is seen in Figure 9Figure 9. Internal connection of the PV-battery . The solar PV module is connected in parallel with the battery ban, whereas charging and discharging current from the battery is controlled by BMS.

In the case of failure, the BMS will disconnect the battery bank from the output terminals and the load. A diode and fuse also were used to provide extra protection for the system from overload and reverse current flow from the battery to PV array.

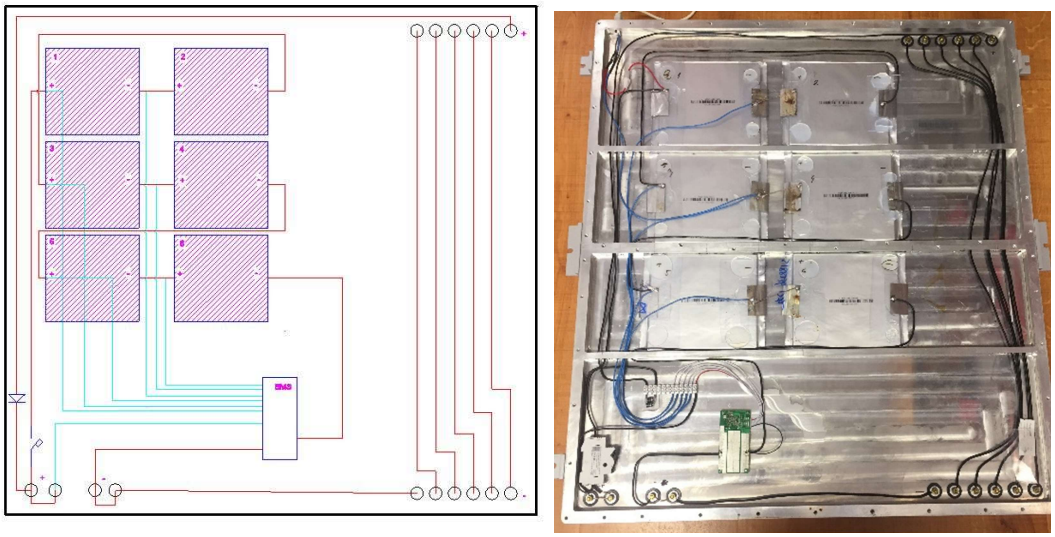

Figure 9. Internal connection of the PV-battery module

Characteristic	Value	Unit
Input charging voltage	25.2	V
Input charging Current	5	A
Maximum input charging current	8	A
Over-current discharge protection per cell	55	A
Over-charge voltage protection per cell delay time of 1.5 s	4.2	V
Depth discharge protection voltage delay time of 1.5 s	2.8	V
Operating temperature range	–20 to +70	ºC

Table 2. Battery management system configuration

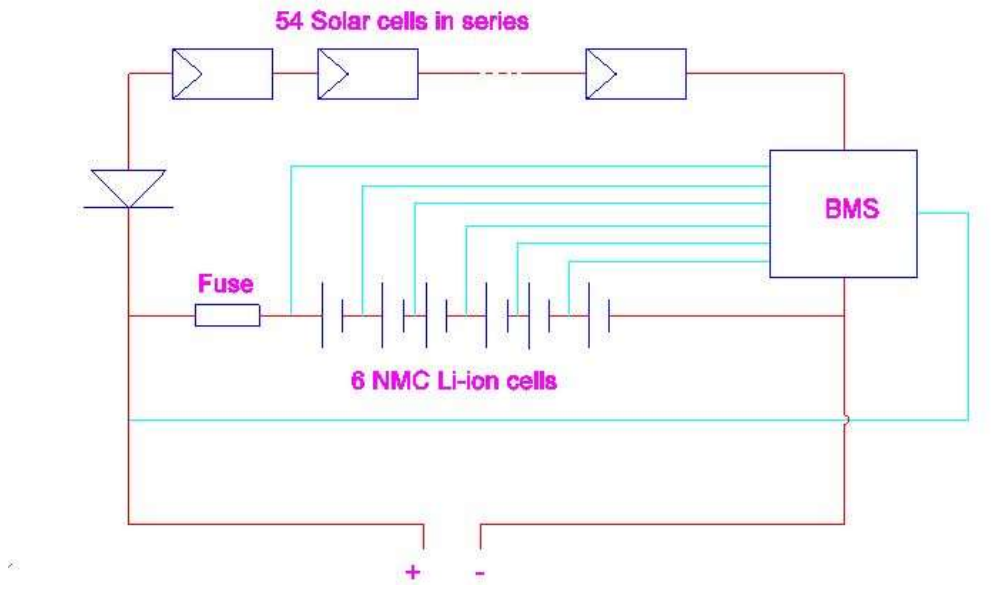

Figure 10. Schematic of the PV-battery module

The batteries were fixed by silicone adhesive to an aluminum cooling profile box for cooling and protection purposes. The prismatic batteries were arranged in a “parallel” configuration concerning the cooling profile. Concerning the efficiency of cooling, it is more

effective than a “serial” arrangement of battery plates. There is a 3 mm air gap between the aluminum cooling box cover of the PV module’s rear side. This gap allows for passive cooling airflow and reduces the temperature of both the cooling profile and the PV module.

The temperature of the aluminum case, the PV module laminate, and the battery pouch was measured using thermocouples. The ambient temperature and intensity of solar radiation were measured by the professional meteorological station at CULS. Characteristics of the PV-battery module discharging process were measured by a setting with the external digital load. All the monitoring data were recorded with a 3 s interval and processed up to test request.

C 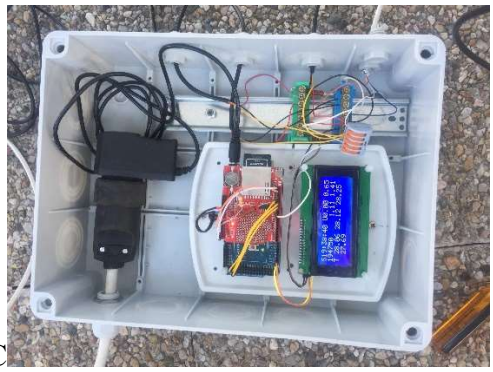

Figure 11. Datalogger box

A prototype of the PV-battery module was installed on the roof of the physics department. The azimuth angle is –50° from the south and the tilt angle is 37°. Because of the fixed support foundation on the roof of our department, the orientation or azimuth angle of

the module cannot be changed. The tilt angle was chosen at the optimal angle to receive most of the solar energy during the year in this location.

Figure 12. Front and rear side of the PV-battery module prototype

Figure 13. Measuring electrical characteristics of the PV-battery module prototype

3.3 TECHNO-ECONOMIC MODEL

A safe and reliable prototype is only half of our task for this research. The ultimate goal is creating a feasible product that can be commercialized. For this purpose, we need to examine the prototype from an economic point of view. Within this research, a techno-economical model was used to evaluate the cost of the module and find out what conditions will make the PV-battery module feasible.

This model simulates the energy production of the module for every hour over a year. This task was solved with the help of PVGIS tools. These tools provide synthetic solar radiation from a satellite; calculate inclined plane radiation; and calculate PV power output with regard to shallow-angle reflection, the effect of changes in the solar spectrum for crystalline silicone, dependence on irradiance, and module temperature.

Energy produced by the PV module is either consumed by the load directly or stored in the battery. The load consumes energy from the module or the battery depending on when it operates.

The model starts by requiring external inputs about the PV module, battery, interesting location, mounting system, components, and other costs. Details of every sub-model are explained in the following sections.

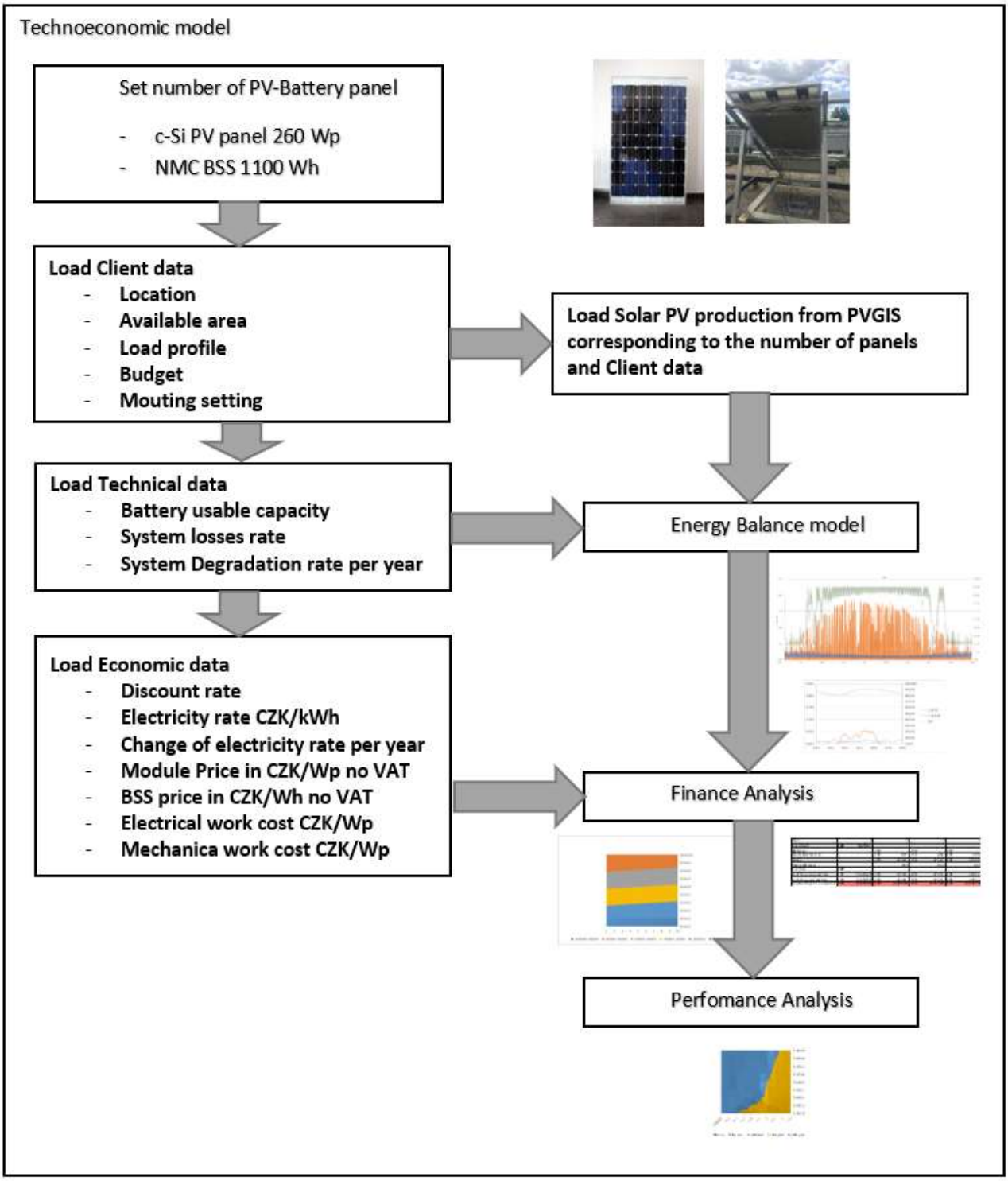

Figure 14. Techno-economic model

3.3.1 Model input

Set initial system size	
	PV size kWp
	BSS size kWh
	Number of PV-battery modules
Load client data	
	Longitude
	Latitude
	Maximum roof area m^2
	Annual energy consumption MWh
	Load profile (choose)
	Budget of client CZK
	Tilt angle
	Orientation
Load technical data	
	Maximum charged capacity BSS kWh
	Minimum charged capacity BSS kWh
	System loss rate
	System degradation rate per year
Load rate data	
	Discount rate
	Exchange rate CZK -> EUR
	Electricity rate CZK/kWh
	Change in electricity rate per year
Load system component prices and costs in CZK	
	Module price in CZK/Wp no VAT
	Inverter price in CZK/Wp no VAT
	BSS price in CZK/Wh no VAT
	Module recycling cost CZK/kg
	Mounting system price CZK/Wp
	Electrical work cost CZK/Wp
	Mechanical work cost CZK/Wp

Table 3. Input parameters

3.3.2 PV energy calculation

PV energy output from the PV module is extracted from the PVGIS tools as shown in Figure 15. PVGIS user interface. The input parameters such as coordination of the installing location, size, and technology of the PV cell, slope, and azimuth of the module are filled in according to the previous section. System loss will be 0% as we will consider the loss separately in the model.

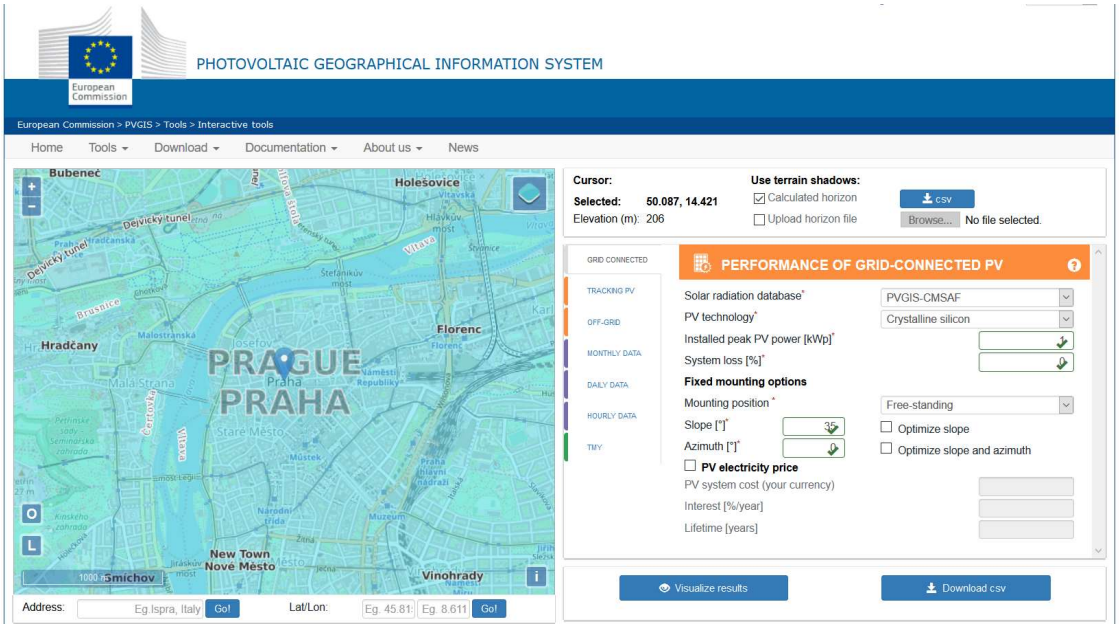

Figure 15. PVGIS user interface

Latitude (decimal degrees)	49.606
Longitude (decimal degrees)	18.005
Elevation (m)	267
Radiation database	PVGIS-CMSAF
Slope	5
Azimuth	87
Nominal power of the PV system (crystalline silicon) (kWp)	1
System losses (%)	0

Table 4. Interested location details

Hour	Date	EPV[1]	G_i[2]	As[3]	Tamb[4]	W10[5]
1	20150101:0055	0	0	0	–5.29	3.31
2	20150101:0155	0	0	0	–4.69	2.89
3	20150101:0255	0	0	0	–4.09	2.46
4	20150101:0355	0	0	0	–3.48	2.04
5	20150101:0455	0	0	0	–3.21	1.95
6	20150101:0555	0	0	0	–2.93	1.86
7	20150101:0655	0	0	0	–2.65	1.77
8	20150101:0755	15.04	26.41	7.6	–2.05	1.66
9	20150101:0855	0.32	6.19	12.98	–1.44	1.55
10	20150101:0955	10.79	21.42	16.34	–0.84	1.45
11	20150101:1055	26.51	39.34	17.38	–0.18	1.48
12	20150101:1155	1.35	8.24	15.98	0.48	1.51
13	20150101:1255	36.95	50.62	12.3	1.14	1.54
14	20150101:1355	13.77	25.26	6.65	0.83	1.71
15	20150101:1455	0	0	0	0.52	1.88
16	20150101:1555	0	0	0	0.21	2.04
17	20150101:1655	0	0	0	–0.28	2.11
18	20150101:1755	0	0	0	–0.76	2.19
19	20150101:1855	0	0	0	–1.25	2.26
20	20150101:1955	0	0	0	–1.85	2.7
21	20150101:2055	0	0	0	–2.44	3.14
22	20150101:2155	0	0	0	–3.03	3.57
23	20150101:2255	0	0	0	–2.86	3.26

Table 5 Sample of PVGIS result

[1] EPV: PV system power (W)
[2] G_i: In-plane irradiance (W/m2)
[3] As: Sun elevation (deg.)
[4] Tamb: Ambient temperature (deg. C)
[5] W10: Wind speed (m/s)

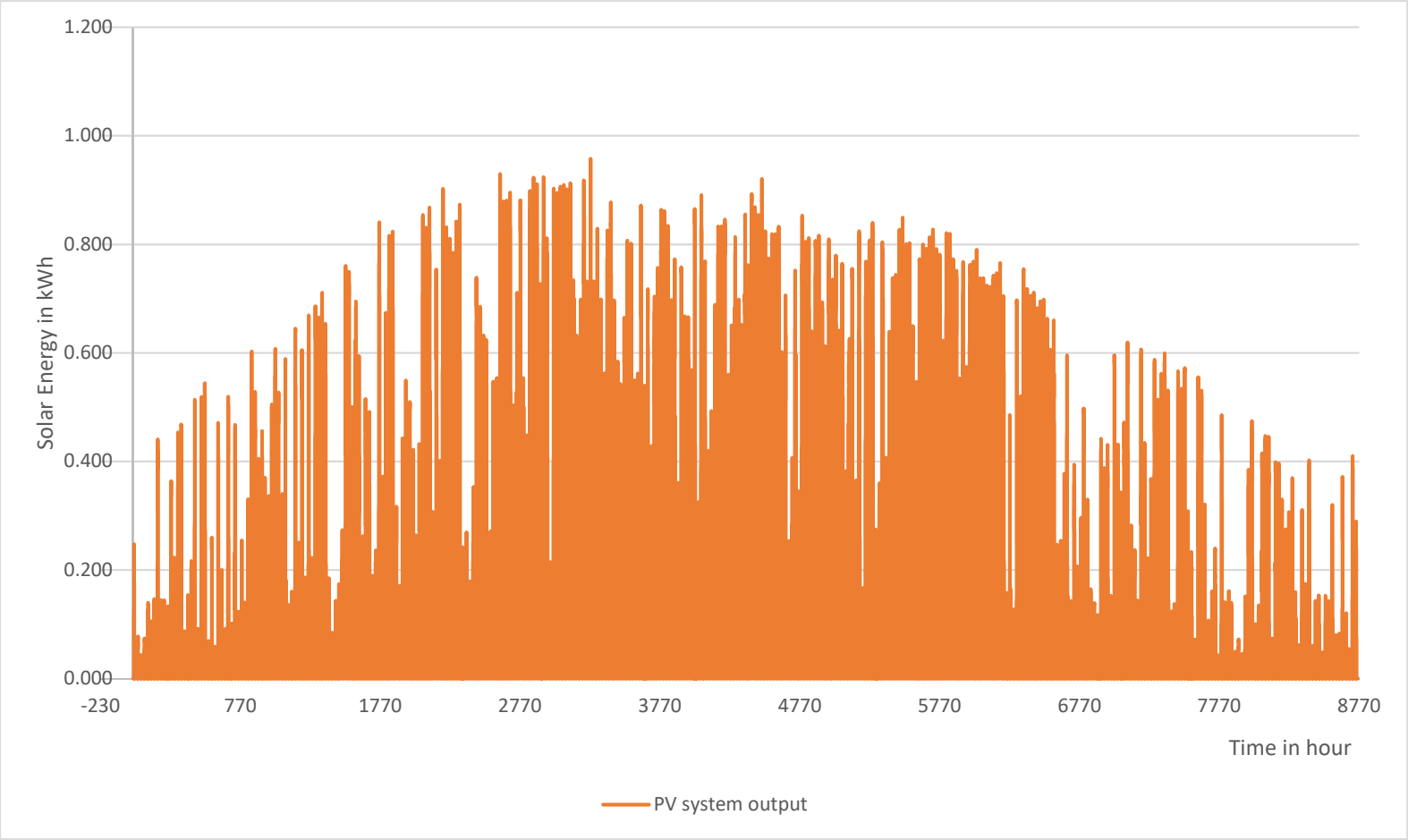

Figure 16. Solar energy output from PVGIS

3.3.3 Energy balance model

For every hour, this following energy balance is calculated to find out the energy flow between PV module, battery, load, and loss. The solar energy output from the PV (E_{PVout}) module is recalculated to eliminate the possible losses caused by the interconnection between the PV module and battery, BMS consumption, and diode loss.

$$E_{\mathrm{PVout}} = E_{\mathrm{PV}}(1 - \text{system losses}) \tag{3.1}$$

The energy difference (E_{diff}) between the output from the PV module and load demand (E_{load}) is calculated in the next step.

$$E_{\mathrm{diff}} = E_{\mathrm{PVout}} - E_{\mathrm{load}} \tag{3.2}$$

Two cases could happen when the energy from the PV module is higher than load demand, so that the system has surplus energy (E_{surplus}).

$$\text{If } E_{\mathrm{diff}} \geq 0 \text{ then } E_{\mathrm{diff}} = E_{\mathrm{surplus}} \tag{3.3}$$

The model continues to evaluate if all of the surplus energy can be charged into the battery, which depends on the battery state of charge from the previous hour. If all of this energy can be charged, then we record this surplus energy as consumed by the system (ΔE_1).

$$\text{If } E_{\text{surplus}} + E_{\text{battery}} = \Delta E_1 \leq E_{\text{battery\_max}}, \text{ then all surplus goes to battery} \quad (3.4)$$

In the case where the battery will be overcharged if all the surplus energy is charged into the battery, the BMS prevents this by cutting the energy flow into the battery when the battery state of charge reaches the designated capacity ($E_{\text{battery\_max}}$). Only the part of the energy (ΔE_2) used to charge the battery is recorded as consumed energy. The rest of the energy (E_{loss}) is listed as losses by the full battery.

$$\text{If } E_{\text{surplus}} + E_{\text{battery}} > E_{\text{battery}_{\text{max}}} \text{ then } \Delta E_2 = E_{\text{battery\_max}} - E_{\text{battery}} \quad (3.5)$$

$$E_{\text{loss}} = \ E_{\text{surplus}} - \Delta E_2; \quad (3.6)$$

In the opposite case, where the load demand is higher than available PV module energy, there is a lack of energy (E_{lack}) in the system.

$$\text{If } E_{\text{diff}} < 0 \text{ then } E_{\text{diff}} = E_{\text{lack}} \quad (3.7)$$

In the first case, the lacking energy is withdrawn from the battery and battery does not reach the minimum state of charge. All of this discharged energy is recorded as consumed energy (ΔE_3).

$$\text{If } E_{\text{battery}} - E_{\text{lack}} = \Delta E_3 \geq E_{\text{battery\_min}}, \text{then all lack comes from battery} \quad (3.8)$$

In the other case, only part of the lacking energy (ΔE_4) is withdrawn because BMS prevents under discharging battery.

$$\text{If } E_{\text{battery}} - E_{\text{lack}} < E_{\text{battery\_min}}, \Delta E_4 = \ E_{\text{battery}} - E_{\text{battery\_min}}; \quad (3.9)$$

After hourly evaluation of energy flow, the model summarizes the yearly results such as total PV production, total self-consumption, and total losses by the full battery.

Total PV production per year in kWh is

$$E_{\text{PV\_total}} = \sum_{i=1}^{8760} E_{\text{PVout\_}i} \quad (3.10)$$

Total self-consumption energy in kWh is

$$E_{\text{self-consumpti}} = \sum_{i=1}^{8760} \Delta E_{1\_i} + \Delta E_{2\_i} + \Delta E_{3\_i} + \Delta E_{4\_i} \quad (3.11)$$

Total energy loss by full-battery per year kWh is

$$E_{loss\_total} = \sum_{i=1}^{8760} E_{loss\_i} \tag{3.12}$$

The self-consumption ratio is

$$r_{self-consumptio} = \frac{E_{self-consumption}}{E_{PV\_total}} \tag{3.13}$$

The self-sufficiency ratio is

$$r_{self-sufficience} = \frac{E_{self-consumption}}{E_{load\_total}} \tag{3.14}$$

3.3.4 Cost calculation model

The total initial investment is the combination of component cost and labor cost. Component cost is the cost of material such as PV cell, sheets of glass for PV module, Al frame, polysiloxane gel, NMC battery cells, Al battery housing profile, and other electrical equipment. Labor costs include electrical works for making the PV-battery modules and wiring internal and external interconnection; mechanical work involves installing the module.

$$\text{Total investment} = \text{Component cost} + \text{Labor cost} \tag{3.15}$$

$$\text{Component cost} = C_{\text{PV panel}} + C_{\text{Battery}} + C_{\text{BMS and other equipments}} \tag{3.16}$$

$$\text{Labor cost} = C_{\text{mechanical}} + C_{\text{electrical}} \tag{3.17}$$

$$\text{Capital expenditure (CAPEX)} = \text{Investment} - E_{\text{self-consumption}} r_{\text{fuel}} \tag{3.18}$$

$$\text{Operational expenditure (OPEX)} = C_{\text{operation and maintenance}} \tag{3.19}$$

Net present value (NPV) is the difference between the present value of cash inflows and the present value of cash outflows over some time. NPV is used in capital budgeting and investment planning to analyze the profitability of a projected investment or project.

$$\text{Net present value} = \sum_{i=0}^{25} \frac{\text{Net cash flow at year } i}{(1 + \text{discount rate})^i} \tag{3.20}$$

The levelized cost of energy (LCOE) is a measure of a power source that allows a consistent comparison of different methods of electricity generation. It is an economic assessment of the average total cost to build and operate a power-generating asset over its lifetime divided by the total energy output of the asset over that lifetime.

$$\text{Levelized cost of energy (LCOE)} = \frac{\sum_0^{25} \frac{\text{CAPEX}_i + \text{OPEX}_i}{(1 + \text{discount rate})^i}}{\sum_0^{25} \frac{E_{\text{self-consumptio }\_i}}{(1 + \text{discount rate})^i}} \tag{3.21}$$

3.3.5 Point calculation model

The technical points are assigned to evaluate the system design under three criteria: self-consumption ratio, self-sufficiency ratio, and grid parity ratio.

- **Point P1: self-consumption ratio**

This point is set to evaluate the suitability of the system for a particular load profile. The self-consumption ratio is high if the load profile distributes mostly during the day when the sun is shining the most, and during the evening the load requires a small amount of energy, which could be supplied by the battery. Each percentage equals 1 point; the minimum point is 0, when none of the PV energy is used; and the maximum point is 100, when all of the PV energy is used in the load.

$$y = 100x \tag{3.22}$$

Where

y is points P1

x is self-consumption ratio

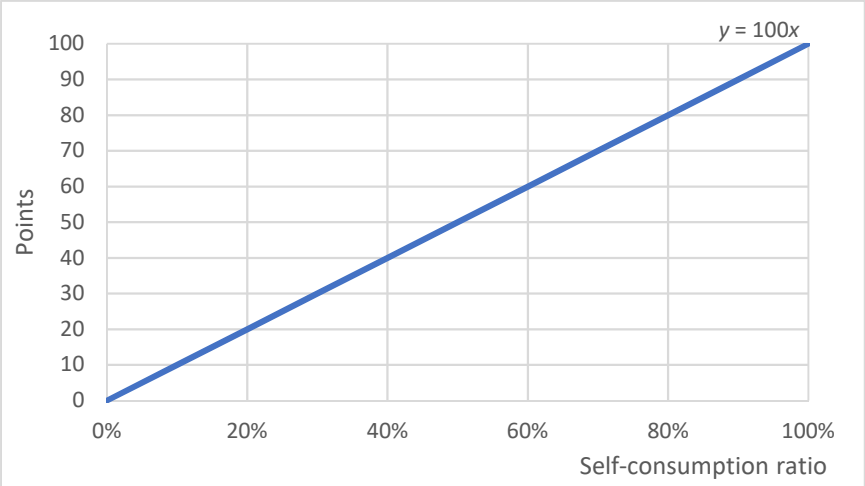

Figure 17. Point P1: self-consumption ratio

- **Point P2: self-sufficiency ratio**

This point is used to evaluate the suitability of the PV module size and battery capacity regarding the particular load demand. A higher point P2 means the PV-battery module could provide sufficient energy for demand. A low point P2 means either the module is inadequate or the added module should be used. Each percentage equals 1 point; the minimum point is 0, when none of the PV energy is used; and the maximum point is 100, when all of the demanded energy is supplied by the PV energy.

$$y = 100x \tag{3.23}$$

Where

y is points P2;

x is Self-sufficiency ratio

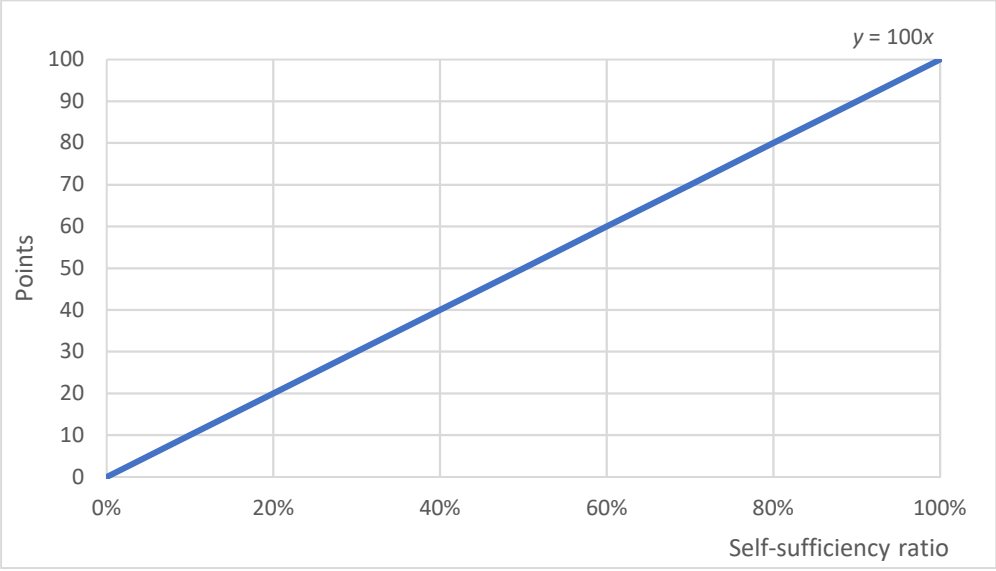

Figure 18. Point P2: self-sufficiency ratio

- **Point P3: grid parity ratio**

This point looks at the financial aspect of the system by comparing the LCOE and the current electricity rate. The formula to calculate point P3 as follows:

$$y = -100x + 200 \tag{3.24}$$

Where

y is Point P3

$$x \text{ is } \frac{\text{LCOE}}{\text{electricity rate}} \tag{3.25}$$

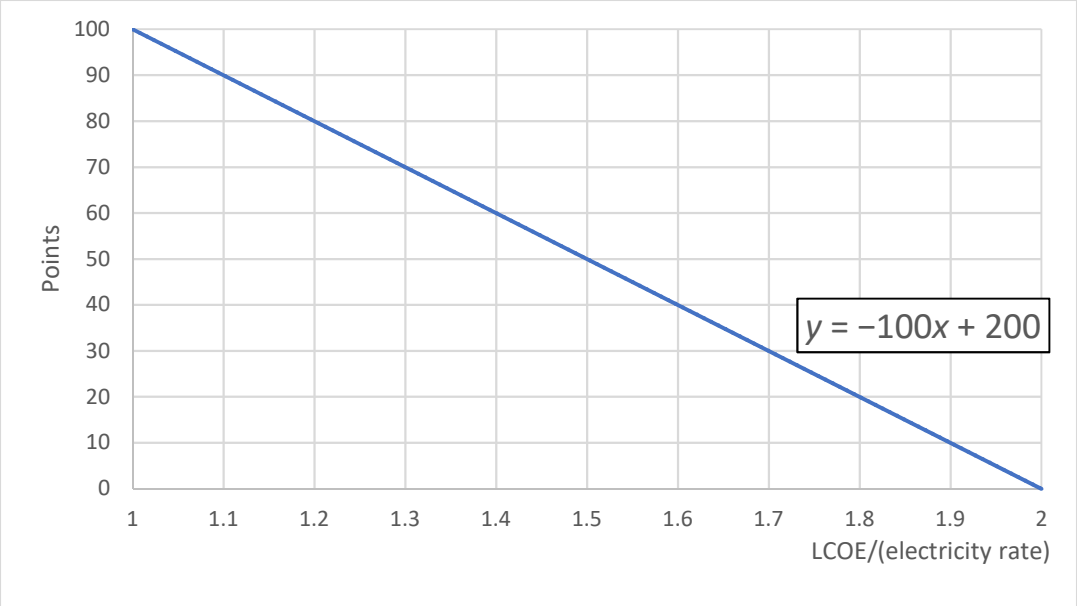

Figure 19. Point P3: grid parity ratio

The minimum point is when the ratio between LCOE and the electricity rate is greater than 2, which means the cost of energy from the PV system is two times higher than the current electricity rate (in an off-grid situation, this is usually the diesel price for genset). When LCOE is lower than the electricity rate, the maximum point P3 will be reached.

3.3.6 Model output

Calculate PV system annual parameters [kWh]	
Total PV production per year in kWh	223.31
Total self-consumption energy in kWh	80.97
Total energy loss because full battery per year in kWh	8.33
Self-consumption ratio	36.3%
Self-sufficiency ratio	81.0%

Table 6. Simulated system performance output

LCOE (CZK/kWh)	CZK 6.10
Payback period no incentive	21
IRR	–3%
NPV	CZK – 5,815.62

Table 7. Simulated financial results

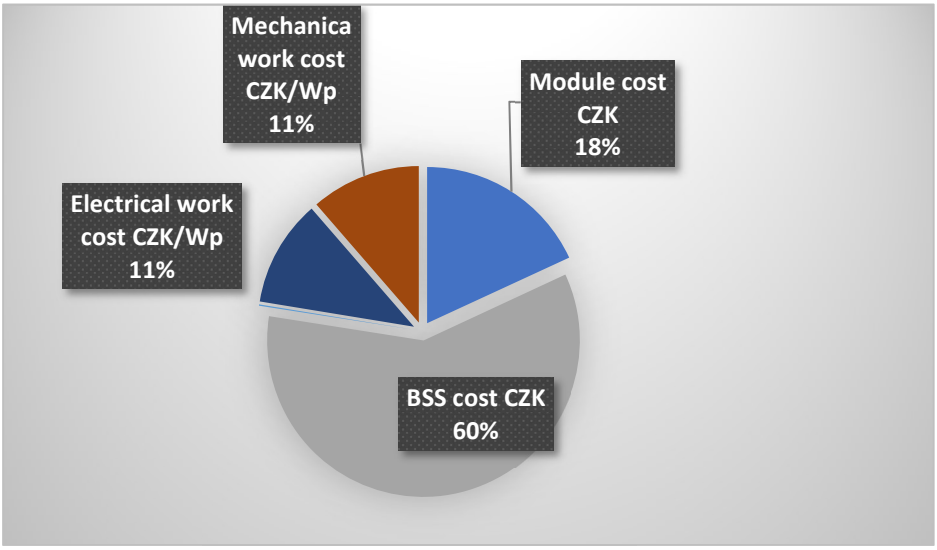

Figure 20. System cost breakdown

Year	0	1	2	3	4	5	6	7	8	9	10
Investment [CZK]	**9,420**										
O&M cost [CZK]		0	0	0	0	0	0	0	0	0	0
Yearly Electric rate [CZK]		4	4	4	4	4	4	4	4	4	4
Saving [CZK]		1,018	1,023	1,028	1,033	1,038	1,043	1,048	1,053	1,059	1,064
Yield kWh/year		254	253	252	251	249	248	247	246	244	243
Cash Flow no incentive [CZK]	-9,420	1,022	1,027	1,032	1,037	1,042	1,047	1,052	1,058	1,063	1,068
Cumulative CF no incentive [CZK]	-9,420	-8,398	-7,372	-6,340	-5,303	-4,261	-3,214	-2,162	-1,104	-41	1,027

Year	11	12	13	14	15	16	17	18	19	20
Investment [CZK]										
O&M cost [CZK]	0	0	0	0	0	0	0	0	0	0
Yearly Electric rate [CZK]	4	4	5	5	5	5	5	5	5	5
Saving [CZK]	1,069	1,074	1,080	1,085	1,090	1,096	1,101	1,107	1,112	1,118
Yield kWh/year	242	241	240	238	237	236	235	234	232	231
Cash Flow no incentive [CZK]	1,073	1,079	1,084	1,090	1,095	1,100	1,106	1,111	1,117	1,122
Cumulative CF no incentive [CZK]	2,101	3,179	4,263	5,353	6,448	7,548	8,654	9,766	10,883	12,005

Table 8. Cash flow of the system during 20 years

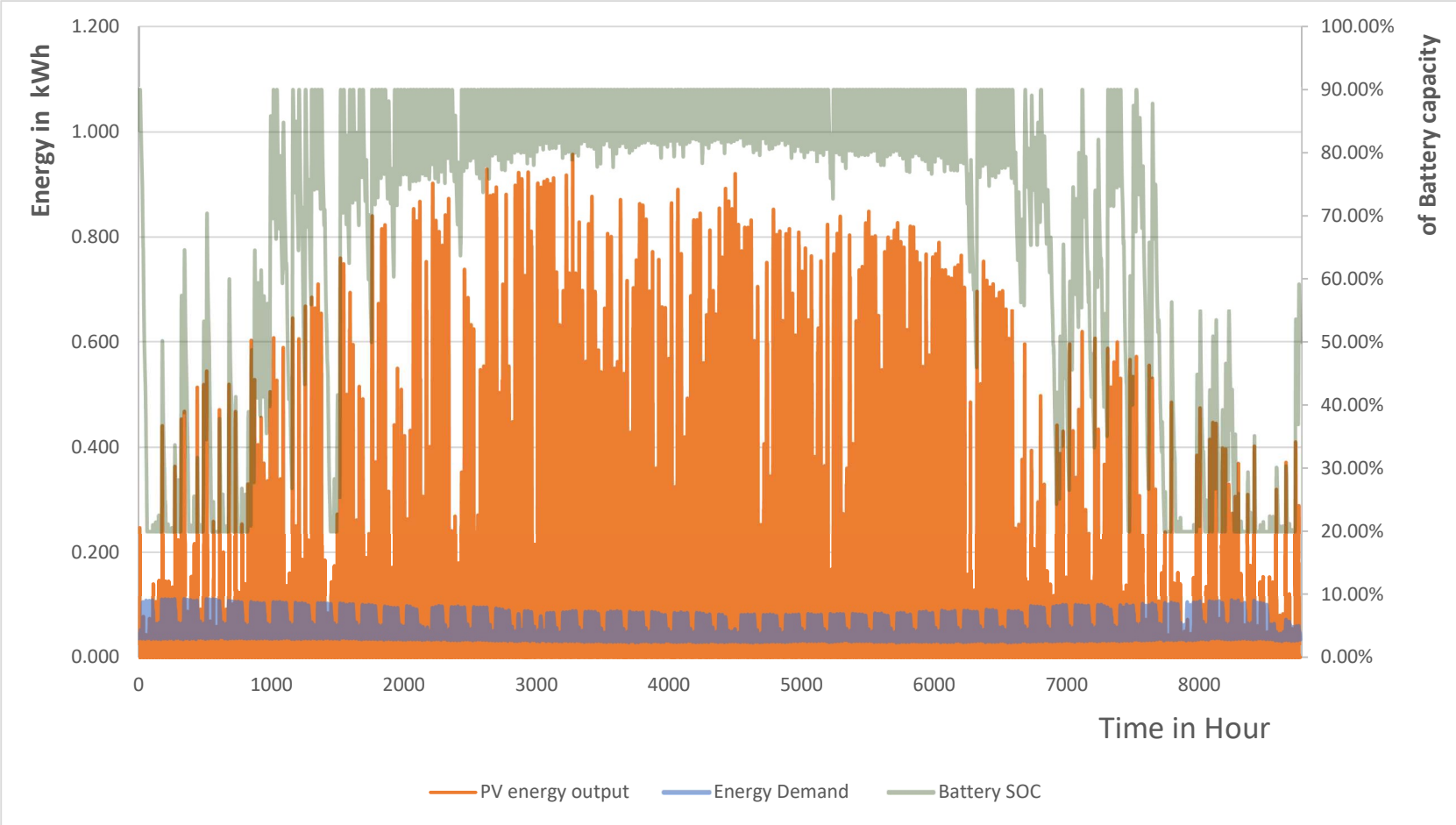

Figure 21. Energy Production and Demand with Battery SOC

Chapter 4. MEASURING RESULTS

4.1 BATTERY TEMPERATURE UNDER HIGH DISCHARGE CURRENT AT NOON WITHOUT THE PV PANEL

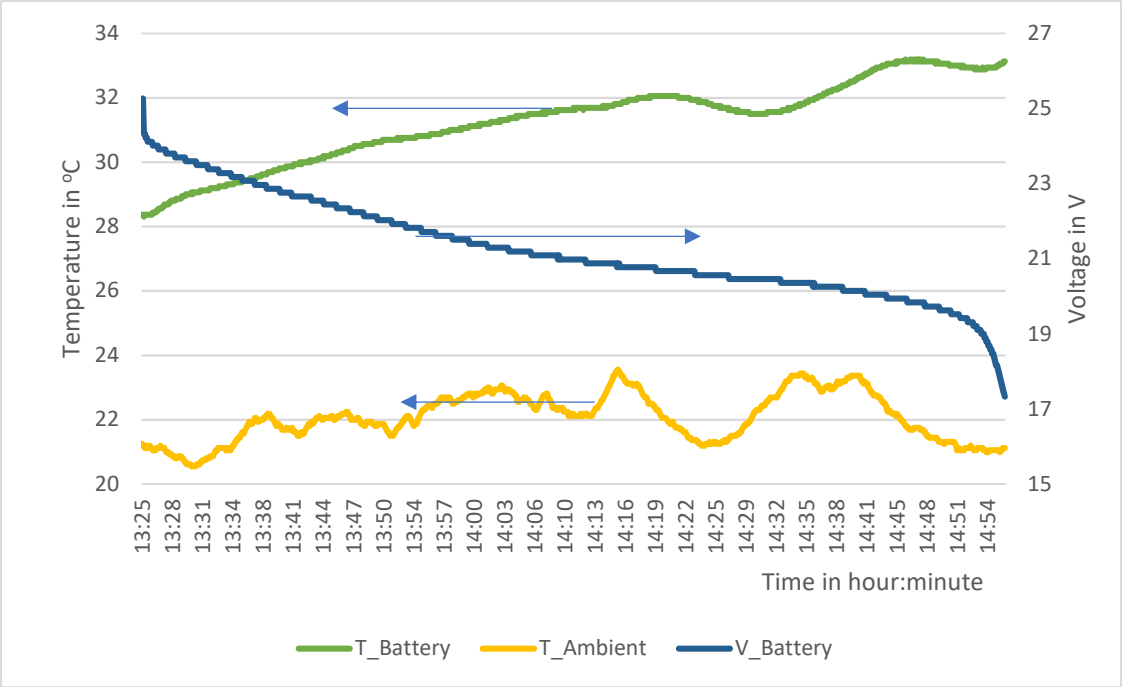

Figure 22. Temperatures and battery voltage during a 30 A constant discharge current without the PV panel

At noon of 30.06.2017, we conducted the test for the system under a constant current discharge of 30 A with the PV panel covered. This test aimed to examine the ability of the system under summer conditions, which is over-temperature. The setting of the test is shown in Figure 8.

The temperature of the battery was affected by the ambient temperature and the discharging time. After 1 h 31 min, the battery temperature increased from 28.31 to 33.19 °C, which means the average battery temperature during the discharging period was 31.26 ± 1.25 °, compared to the average ambient temperature of 22.07 ± 0.74 °C.

Under minute-long intervals, the rate of change in the battery and ambient temperature were investigated.

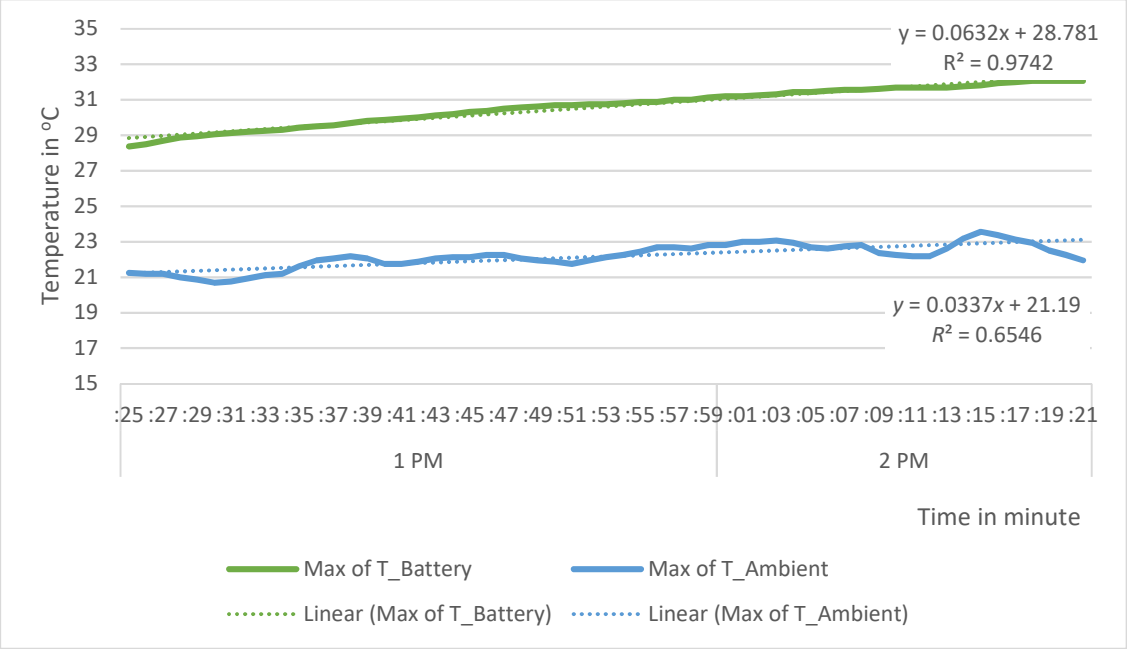

Figure 23. Trend lines for the high discharge current test without the PV panel

Battery temperature increased about 0.06 °C every minute compared to ambient temperature increasing only 0.03 °C per minute.

4.2 BATTERY TEMPERATURE UNDER HIGH DISCHARGE CURRENT AT NOON WITH THE PV PANEL

This test was conducted at noon on 04.07.2017. It was the same test as before only the PV panel was uncovered. The time of testing was 1 h 43 min. Battery temperature increased from 28.12 to 33.88 °C, which means the average battery temperature during the discharging period was 32.01 ± 1.21 °C. Compared to the average ambient temperature, which was 23.85 ± 0.58 °C.

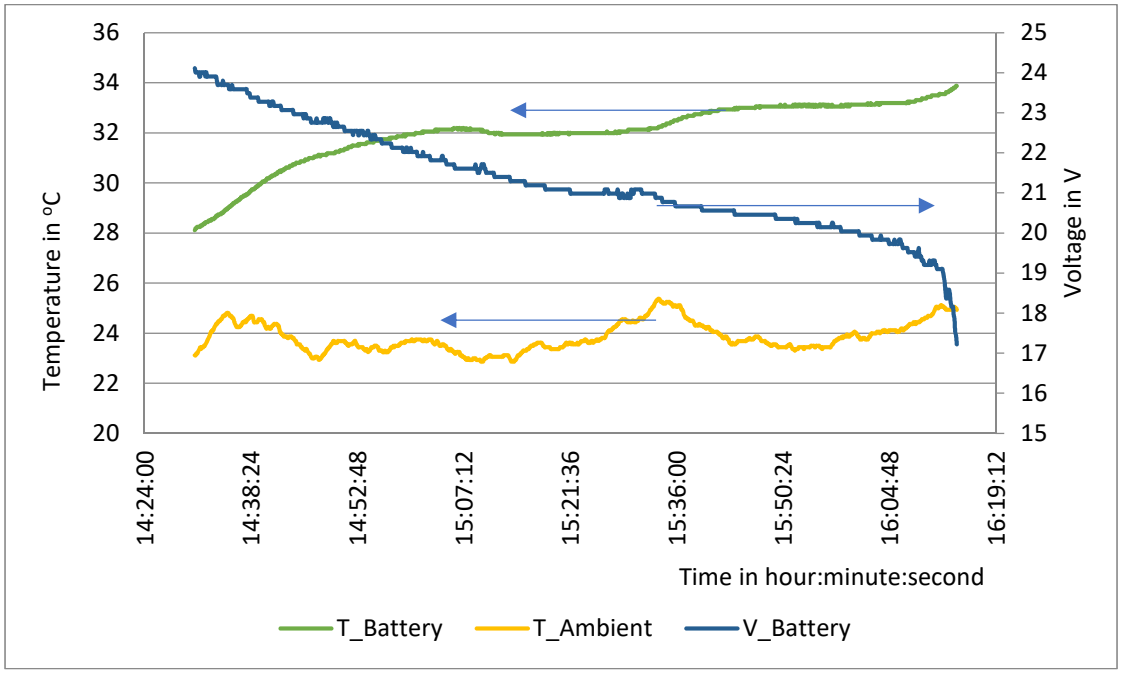

Figure 24. Temperatures and battery voltage during a 30 A constant discharge current with the PV panel

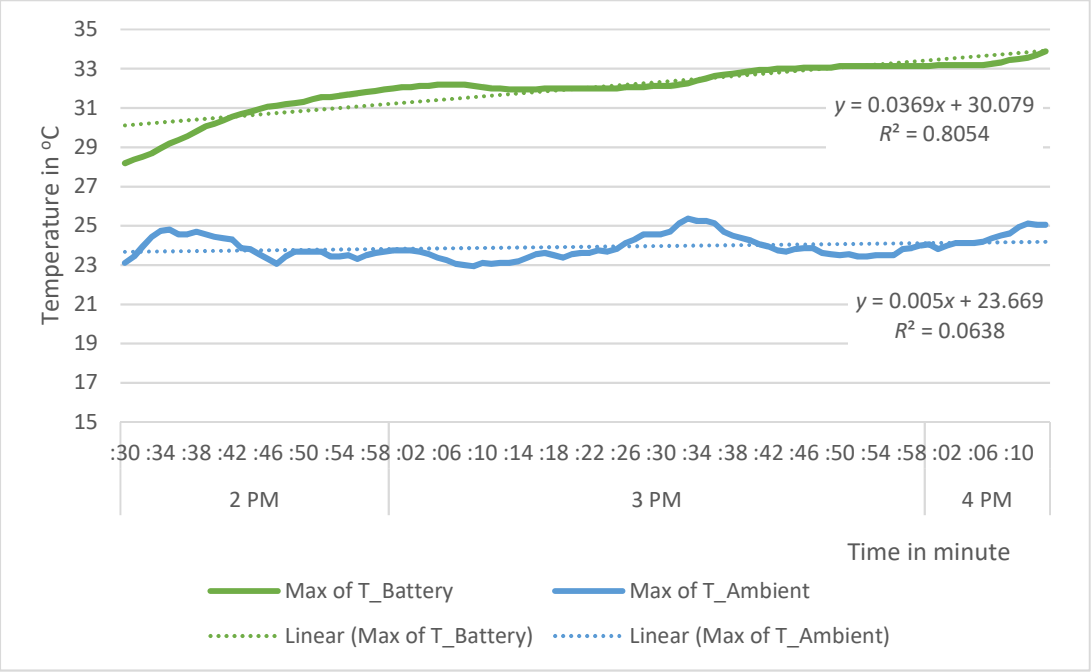

Figure 25. Trend lines for high discharge current test with the PV panel

The rate of change in the battery and ambient temperatures were investigated under minute-long intervals. Battery temperature increases about 0.03 °C every minute compared to ambient temperature, which increased only 0.005 °C per minute.

4.3 LONG-TERM MEASUREMENT OF TEMPERATURE

The next test conducted was to observe whether the cooling profile is able to keep the battery temperature inside the range of a safe and operating temperature. The maximum allowed battery temperature is 70 °C.

Figure 22 shows the maximum daily recorded temperature data from the lithium battery and the ambient temperature over a year of operation. The system was put in charging mode during the day and discharge during the night via a time relay. The battery was discharged only after sunset and discharged all of its capacity. The red curve dT Bat-Amb shows the temperature difference between these two temperatures. The maximum difference between them is 14.75 °C, which is when the ambient temperature is 33.63 °C. The correlation between battery temperature and ambient temperature is investigated in Figure 26.

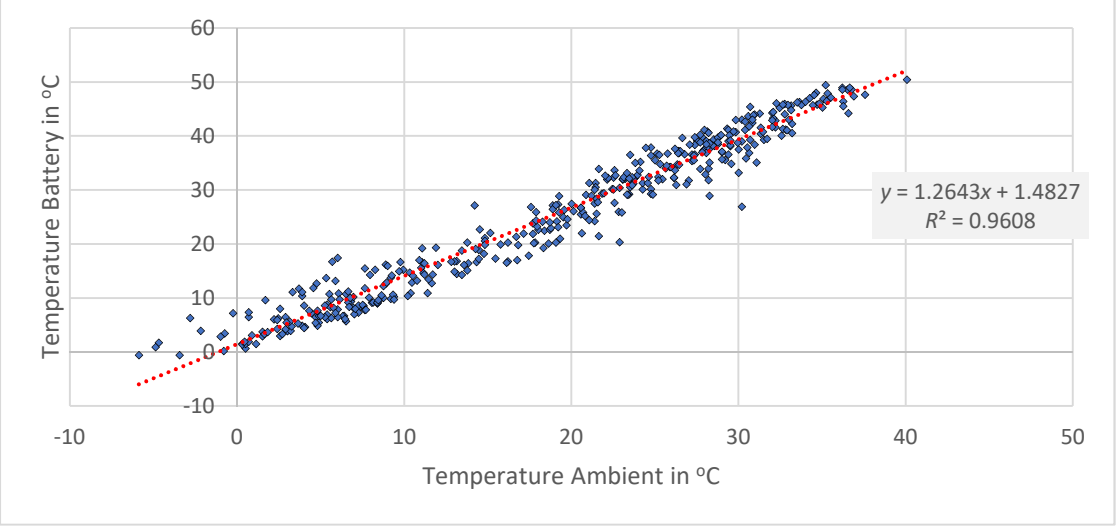

Figure 26. The correlation between battery temperature and ambient temperature

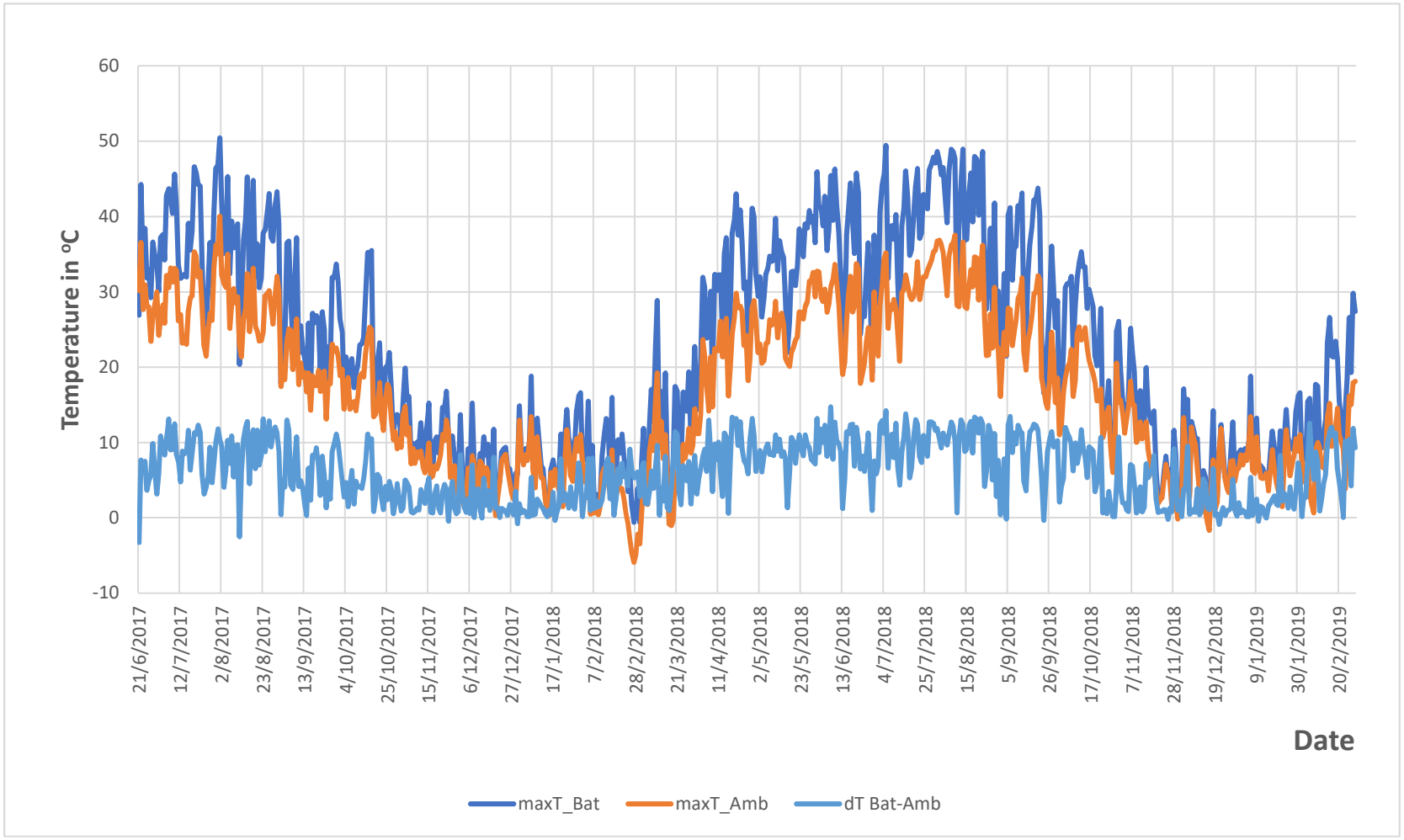

Figure 27. Long-term temperature measurement

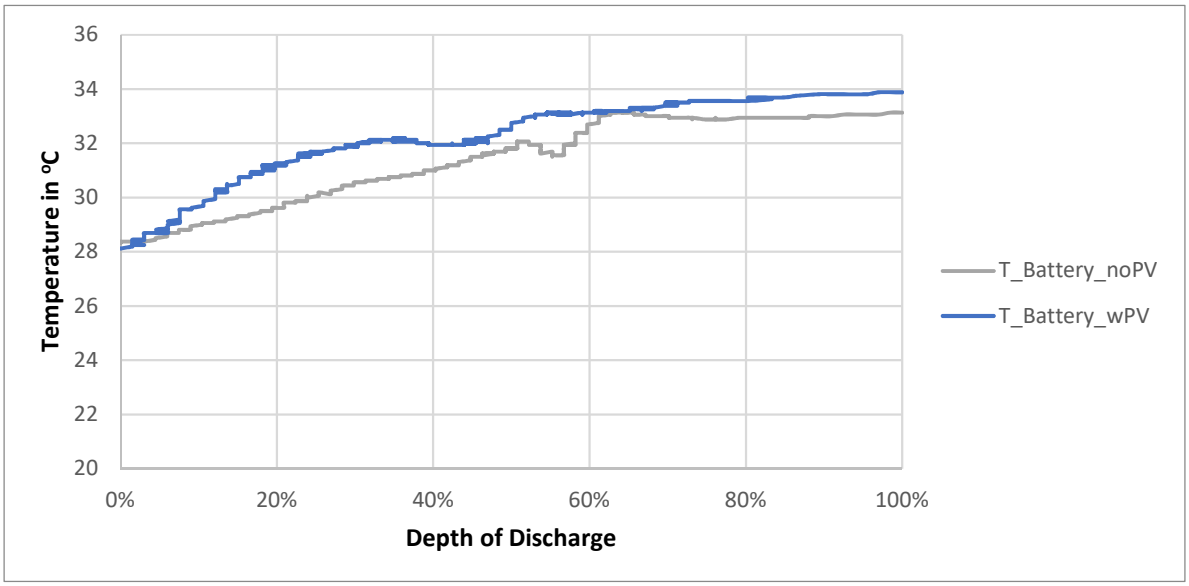

Figure 28. Temperature changing vs. depth of discharge (DOD)

The temperature of the battery during the discharge process experienced a temperature decrease period when DOD about 40–60%. In the initial period, where DOD < 40%, the rate of temperature generation is higher than in the latter period, where DOD > 60%.

After two tests with high current discharge, we observed that the battery temperature increased at a rate of 0.03 °C per minute higher than the ambient temperature. The results show that after the battery is fully discharged (1 h 43 min at 30 A), the temperature will be 3.09 °C higher than the ambient temperature.

Chapter 5. SIMULATION RESULTS

As discussed in the Scope and Objectives chapter, simulation of the system using the PV-battery module is helps us understand the feasibility of the system.

The default input for the simulation is shown in the following table unless it is stated otherwise in the analysis.

Set initial system size		
	0.26	PV size kWp
	1.1	BSS size kWh
	1	Number of PV-battery modules
Load client data		
	50.129	Longitude
	14.374	Latitude
	1000	Maximum roof area m^2
	0.1000	Annual energy consumption MWh
	TDD1	Load profile (choose)
	10000000	Budget of client CZK
	37	Tilt angle
	-50	Orientation
Load technical data		
	90%	Maximum charged capacity BSS kWh
	20%	Minimum charged capacity BSS kWh
	15%	System loss rate
	0.50%	System degradation rate per year
Load rate data		
	7%	Discount rate
	CZK 25.20	exchange rate CZK -> EUR
	CZK 4.00	Electricity rate CZK/kWh
	1.00%	Change in electricity rate per year
Load system component prices & costs in CZK		
	CZK 6.55	Module price in CZK/Wp no VAT
	CZK -	Inverter price in CZK/Wp no VAT
	CZK 5.04	BSS price in CZK/Wh no VAT
	CZK 0.60	Module recycling cost CZK/kg
	CZK -	Mounting system price CZK/Wp
	CZK 4.00	Electrical work cost CZK/Wp
	CZK 4.12	Mechanical work cost CZK/Wp

Table 9. Default input for the simulation

5.1 LOAD PROFILES

The drawback of a PV system is sun availability. Sunlight is only available during a certain period during the day and this period changes with the time of the year and location. In the case of an off-grid system, this is a more serious problem that requires carefully designing the system to ensure power availability. A normalized load profile defines how an electricity customer uses electricity over time regarding peak power. In this work, four types of load profile are investigated:

- **TDD1** is similar to typical load profile in the Czech Republic (OTE, 2018)
- **TDD6** warehouse is similar to a warehouse demand that gradually increases in the morning, is stable during working hours, and drops at night
- **TDD7** hotel is similar to hotel energy demand with peaks at 6 AM, 4 PM, and 8 PM
- **TDD8** custom load profile is made to investigate the worst situation when the load is used during the night from 6 PM to 6 AM the following morning.

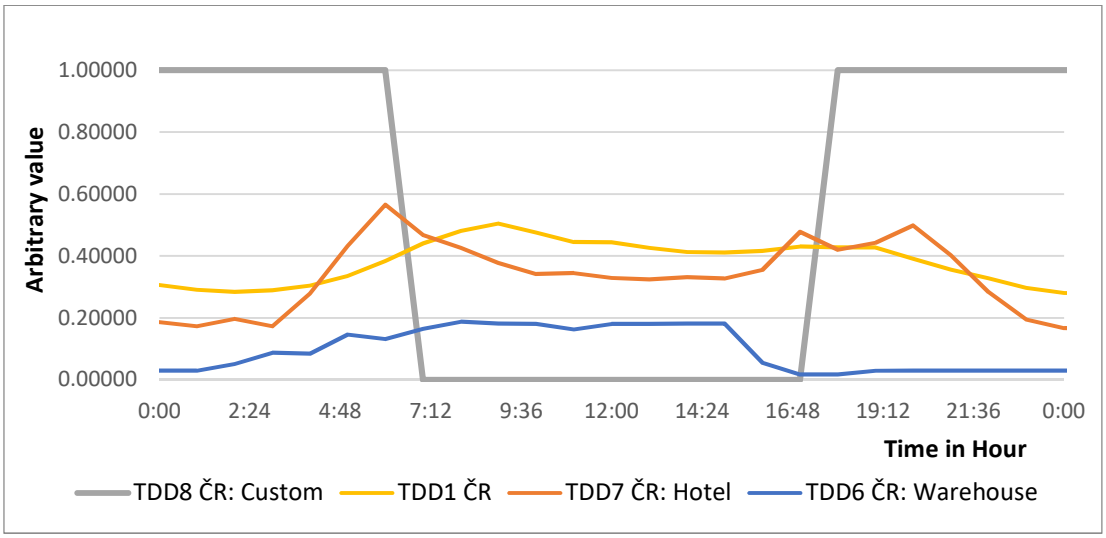

Figure 29. Normalized daily load profile

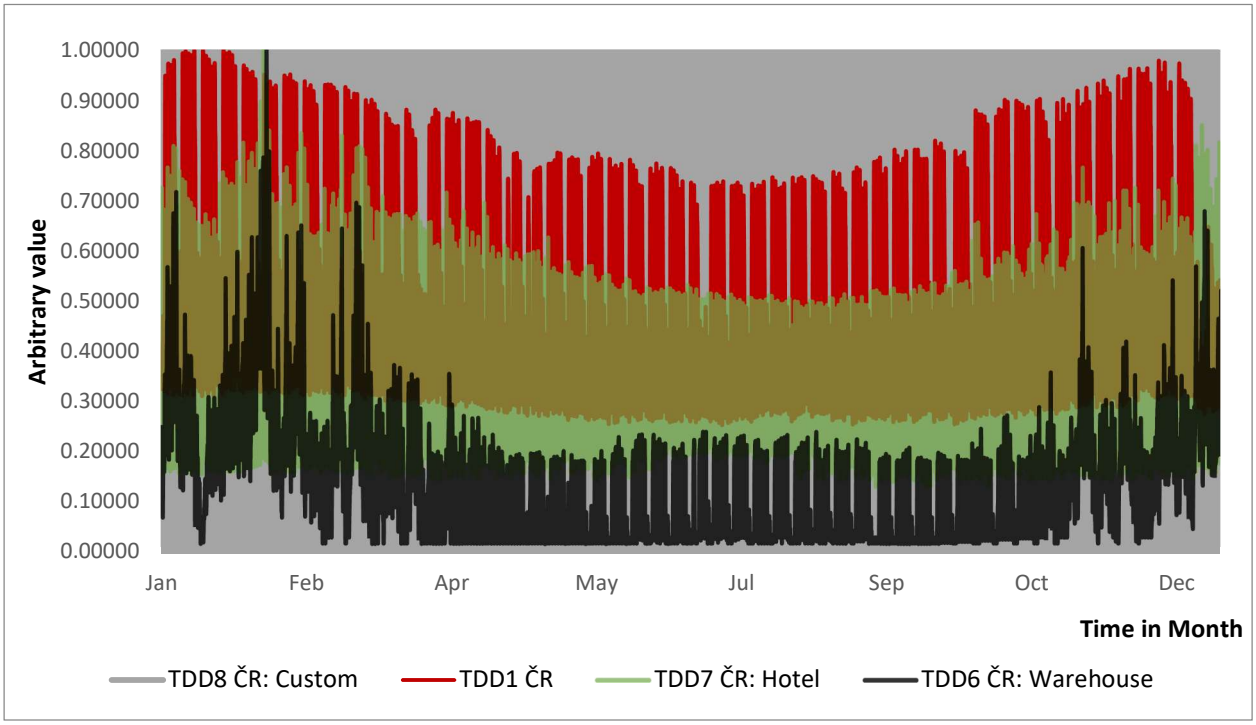

Figure 30. Normalized yearly load profile

Another factor effecting the system operation is the change in load profile by season of the year. In the northern sphere, the winter time from October to February will have low sun irradiation, shorter days, and lower temperature; this leads to higher energy consumption during winter for lighting and heating purposes. This effect is seen in the case of the TDD6 warehouse load profile, when the energy consumption in January and February on some days is three times higher than in the summer. In the case of TDD7 hotel, the difference is not that strong because the energy usage throughout the year is similar. TDD1 as a typical load for the Czech Republic is even more stable during the year, the significant low load demand during the weekend appears as a pattern during the year. The TDD8 custom is kept the same all year.

5.2 EFFECT OF LOAD SIZE ON SELF-SUFFICIENCY RATIO UNDER DIFFERENT LOAD PROFILE

For an off-grid solar system, a high self-sufficiency ratio is a crucial parameter. The system must have high availability so it can supply energy for a load anytime that is necessary. Figure 31 shows how annual energy demand could effect a system with single PV-battery module with different load profiles. Clearly, except for the warehouse, all other load profiles maintain their self-sufficiency ratios at greater than 90% when annual energy demand is lower than 0.1 MWh (100 kWh) per year.

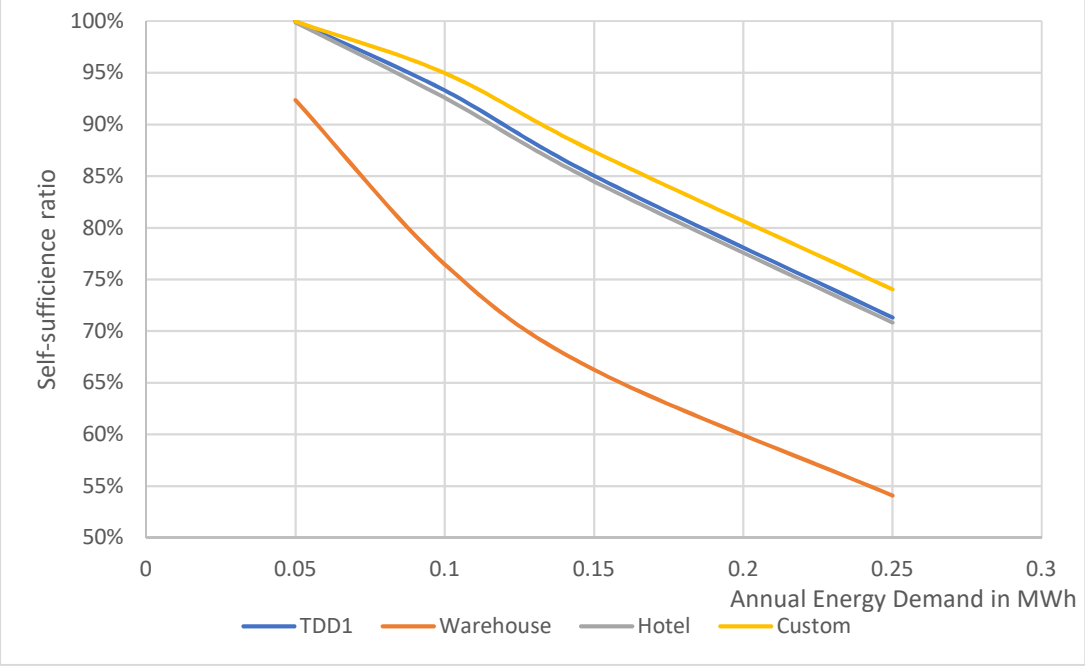

Figure 31. Effect of load size on the self-sufficiency ratio under different load profiles

After the analysis, recommendations are made using the following:

- One PV-battery module is suitable to supply a load with annual energy demand lower than 100 kWh. Higher energy demand the probability of energy shortage increases.
- In the case of high load demand during the winter, the self-sufficiency ratio is low even with low load demand. For that reason, this module is not suitable to use in application require high winter load.
- The next analysis is conducted to further understand the effect of different load profiles on the system behavior. An annual energy consumption of 0.1 MWh is used during this analysis to keep the self-sufficiency ratio greater than 90%.

5.3 EFFECT OF LOAD PROFILE ON SYSTEM UTILITY

Table 10 shows the results of the simulation with different load profiles. Simulation is made with 1 PV-battery module, and the annual energy consumption is 100 kWh.

	TDD1 ČR	Warehouse	Hotel	Custom
Annual energy demand in kWh	100	100	100	100
Total PV production per year in kWh	268.46	268.46	268.46	268.46
Total self-consumption energy in kWh	93.29	76.47	92.58	94.97
Total energy loss because of full battery per year in kWh	11.28	6.92	11.71	16.38
Self-consumption ratio	34.8%	28.5%	34.5%	35.4%
Self-sufficiency ratio	93.3%	76.5%	92.6%	95.0%
LCOE	5.29	6.46	5.33	5.2
Total Points	223	177	221	227
NPV in CZK	–5,273	–6,013	–5,305	–5,200

Table 10. Effect of load profile on system utility

The same total PV production for all cases is 268.46 kWh per year. Total self-consumption energy is highest in the case of the custom load profile and lowest in the case of warehouse load; this could be explained by two reasons. The first reason is the peak load demand in the warehouse is much higher than in all other cases. This peak load happens during the day when the battery has not fully charged, which lead to a lack of energy. The second reason is peak load demand occurs during winter, and during summer the energy demand is significantly lower, which worsens the self-consumption ratio because of energy not being used.

In the cases of TDD1 and hotel, although there is a difference in consumption during winter and summer, the effect on the results is insignificant. In both cases, the self-consumption ratio is about 34% and the self-sufficiency ratio is about 93%. The result in the TDD1 case is slightly better because of the weekend leave, allowing the battery time to recharge.

The interesting case is with the custom load profile. As stated previously, this load profile is expected to be the worst case; however, the result shows the opposite indication. The reason is because of the low peak load demand and relatively high capacity battery, which could supply most of the needed energy during the night.

After the simulation with different load profiles, we have several recommendations for suitable application of PV-battery module:

- The system operation is strongly affected by the peak load demand; the best case is when the difference between the peak load and other times is small. High peak load occurring during winter time might lead to low self-consumption and self-sufficiency ratios.
- Using a pattern with some resting days for the battery to recharge will slightly increase the system utilization.
- Large battery capacity will improve the system's self-consumption ratio and self-sufficiency ratio.

5.4 SENSITIVITY ANALYSIS OF POINTS REGARDING DIFFERENT SIZES OF BATTERY CAPACITY

Following the previous recommendation about the large battery capacity will improve the system utilization. This sensitivity analysis of points regarding the different sizes of battery capacity is performed to find the suitable battery size. All the input parameter but the battery capacity are kept as default. Higher points indicate better system utilization.

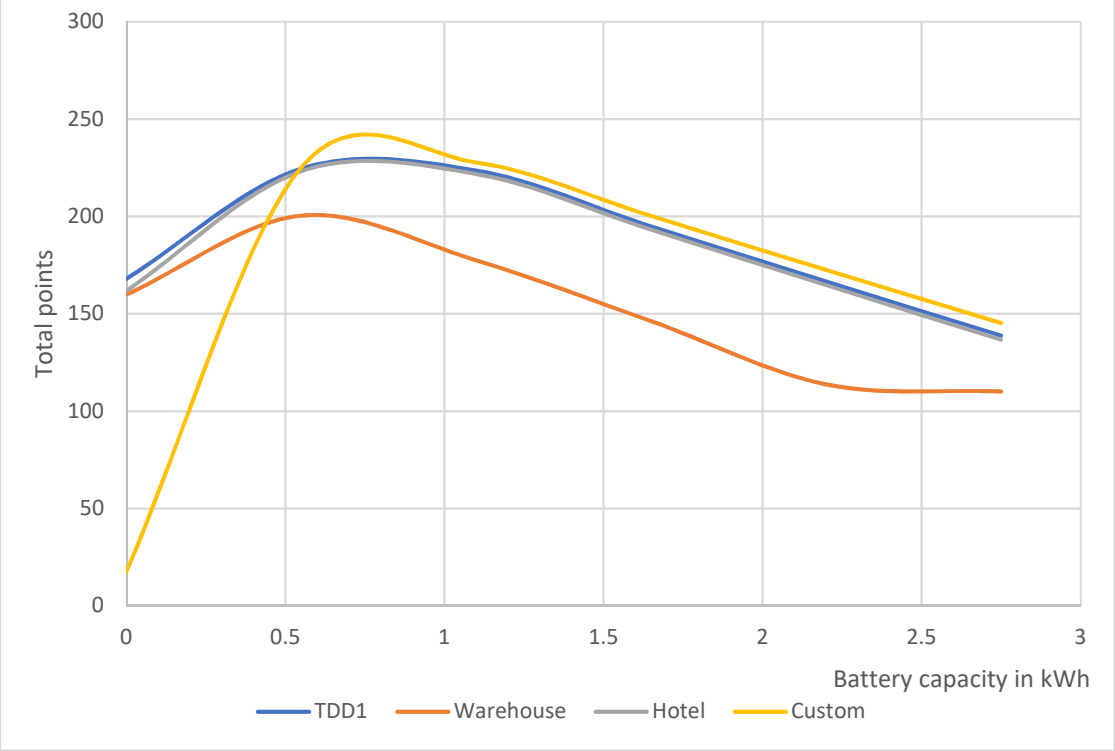

Figure 32. Effect of battery capacity on system total points

Figure 32 shows the effect of battery capacity on system total points under different load profiles. The highest points are achieved with a battery capacity between 0.5 and 1 kWh. When the battery capacity is lower than 0.5 kWh, the total points drop because load demand during the night is not satisfied. On the opposite side, if the battery capacity is larger than 1 kWh, then total points drop because of higher LCOE and system cost.

Our prototype is equipped with a 1 kWh lithium ion battery which lies in the optimal battery capacity range. This result proves that our design is appropriate and suitable for using as a package. The next step we analyze the PV-battery module as a compact system and investigate the situation when more than one module is used.

5.5 SENSITIVITY ANALYSIS OF ANNUAL CONSUMPTION AND SYSTEM SIZE

This analysis is made to understand how the system behaves when annual energy demand is higher and more PV-battery modules must be used. We use load profile TDD1 for this analysis. The annual energy demand from 50 kWh to 50 MWh per year is simulated corresponding to a system size of 1 to 100 PV-battery modules. Two indicators total points and NPV is investigated to evaluate the feasibility of system.

Table 11 shows the total points could be archived when varying annual energy consumption and several modules. Figure 33 shows a rapid increment of points for higher annual energy consumption when using single PV-battery module. The maximum number of points is reached for single PV-battery module to supply a load demand of 0.5 MWh per year. If the number of modules is 5 then maximum points reach with 5 MWh per year load demand. This peak become flatten with more modules used in the system. If more modules are used than necessary the points will reduce and stable at about 200 points because the self-sufficiency ratio is maximum but self-consumption ratio and grid parity ratio decrease with system size.

Table 12 shows the net present value that could be achieved when annual energy consumption is varied and several modules are used. Similar to the total points, positive NPV appears for the system using 1 PV-battery module for at least 0.5 MWh per year. Unlike the points, NPV is not reduce when the load demand increase because the same amount of energy saving. Each module could provide maximum NPV about CZK 2400 after 20 years of operation.

However, as discussed in Section 5.2, using 1 PV-battery panel to supply for an annual energy demand greater than 0.1 MWh per year will lead to a self-sufficiency ratio lower than 90%. For an off-grid system, this could be an undesired situation. To find a solution to this problem, we analyzed the effect of the electricity rate on the system feasibility in the next section.

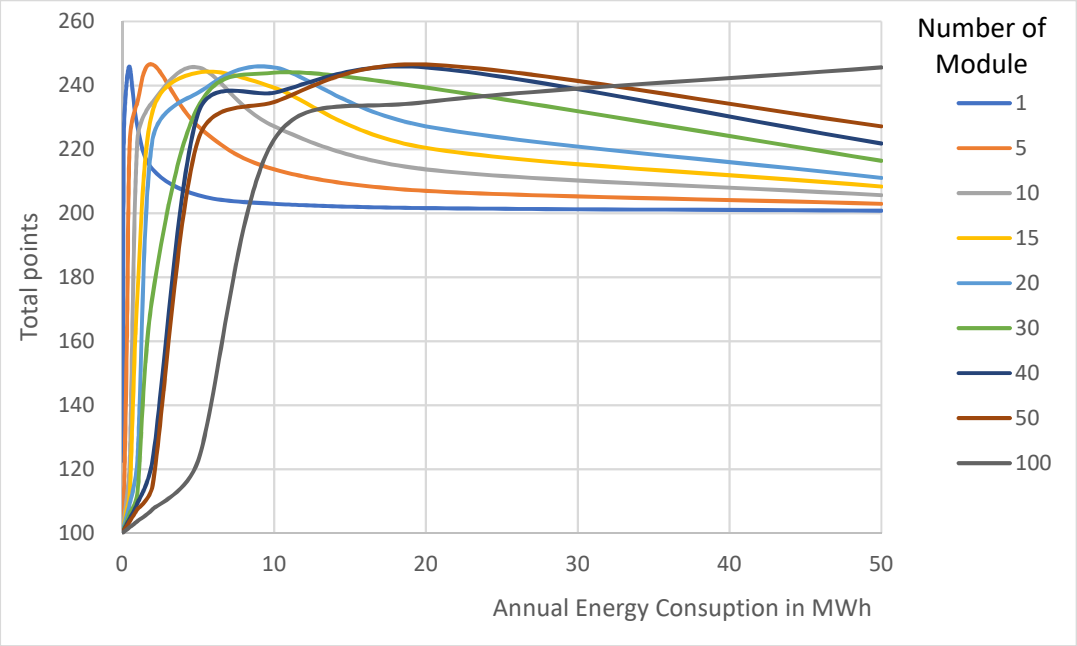

Figure 33. Point of performance depends on annual energy consumption and system size

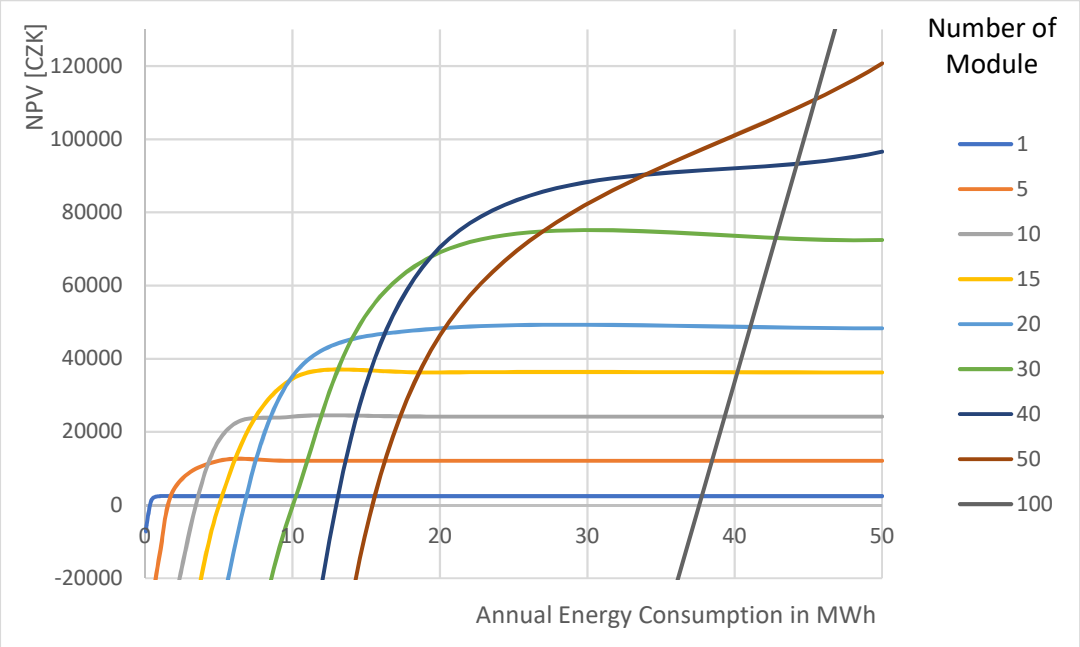

Figure 34. NPV depends on annual energy consumption and system size

Number of modules / Annual energy consumption MWh	**1**	**5**	**10**	**15**	**20**	**30**	**40**	**50**	**100**
0.05	123	104	102	101	101	101	100	100	100
0.1	223	107	104	102	102	101	101	101	100
0.3	241	158	111	107	106	104	103	102	101
0.5	246	223	123	112	109	106	105	104	102
1	227	235	223	174	123	112	109	107	104
2	214	247	235	232	223	174	123	115	107
5	206	227	246	244	238	233	231	223	123
10	203	214	227	239	246	244	238	235	223
20	202	207	214	220	227	239	246	247	235
50	201	203	206	208	211	216	222	227	246

Table 11. Points depend on annual consumption and system size

Number of modules / Annual energy consumption	1	5	10	15	20	30	40	50	100
0.05	-7,177	-44,856	-91,955	-139,054	-186,153	-280,351	-374,549	-468,747	-939,738
0.1	-5,274	-42,659	-89,758	-136,857	-183,956	-278,154	-372,352	-466,550	-937,540
0.3	-572	-33,918	-80,968	-128,067	-175,166	-269,364	-363,562	-457,760	-928,751
0.5	1,806	-26,552	-72,178	-119,277	-166,376	-260,574	-354,773	-448,971	-919,961
1	2,459	-13,099	-53,149	-97,893	-144,402	-238,600	-332,798	-426,996	-897,987
2	2,459	4,680	-26,244	-63,744	-106,344	-195,831	-288,850	-383,048	-854,039
5	2,459	12,113	17,653	-96	-31,653	-101,801	-179,826	-265,928	-722,194
10	2,459	12,114	24,179	34,557	35,260	-238	-63,351	-131,403	-531,902
20	2,459	12,114	24,183	36,251	48,313	69,069	70,473	46,394	-262,853
50	2,459	12,114	24,183	36,251	48,320	72,456	96,593	120,715	176,115

Table 12. NPV depends on annual consumption and system size

5.6 SENSITIVITY ANALYSIS OF ELECTRICITY RATE AND SYSTEM SIZE

Electricity rate is an important parameter in determining the feasibility of the system. This analysis shows how this price of electricity could affect the system size and NPV. The simulation used TDD1 with annual energy consumption is 0.5 MWh as inputs. The electricity rate is varied and other parameters is kept as default.

Table 13 shows how NPV depends on the electricity rate and a number of the module. These results show that when the electricity rate or fuel cost increase, more modules could be used. In the current case of an electricity rate CZK 4 per kWh, when the annual consumption is 0.5 MWh per year and we use 1 PV-battery module, then the self-sufficiency ratio is 50.9% and NPV is CZK 1806. If the electricity rate increases to CZK 8 per kWh, we can use 4 PV-battery modules to increase the self-sufficiency to 89.6% and NPV is CZK 1796.

In off-grid application, diesel generator is a common source of electricity. The increasing price of fuel and inconvenient noise, smell is motivation for user to change into renewable energy.

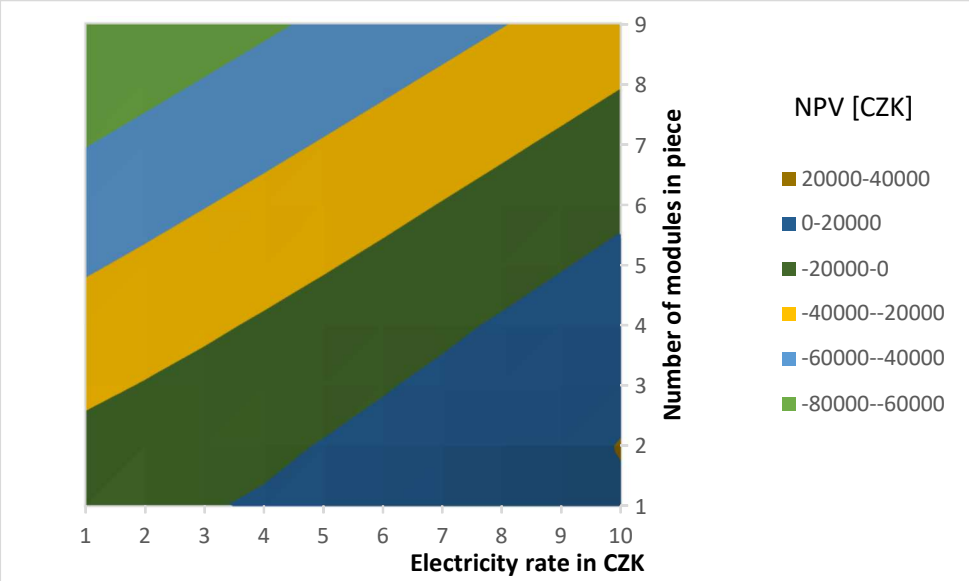

Figure 35. NPV depends on the electricity rate and system size

Number of modules / Electricity rate	1	2	3	4	5	6	7	8	9
CZK 1	–6,613	–14,911	–23,729	–32,745	–41,962	–51,222	–60,542	–69,893	–79,273
CZK 2	–3,807	–10,982	–19,199	–27,810	–36,825	–45,924	–55,146	–64,427	–73,768
CZK 3	–1,000	–7,053	–14,669	–22,876	–31,689	–40,627	–49,749	–58,961	–68,263
CZK 4	1,806	–3,124	–10,139	–17,941	–26,552	–35,330	–44,353	–53,495	–62,758
CZK 5	4,613	805	–5,609	–13,007	–21,415	–30,032	–38,956	–48,029	–57,254
CZK 6	7,419	4,734	–1,079	–8,073	–16,278	–24,735	–33,559	–42,563	–51,749
CZK 7	10,226	8,662	3,451	–3,138	–11,141	–19,438	–28,163	–37,097	–46,244
CZK 8	13,032	12,591	7,981	1,796	–6,004	–14,140	–22,766	–31,631	–40,739
CZK 9	15,839	16,520	12,512	6,731	–868	–8,843	–17,370	–26,165	–35,234
CZK 10	18,646	20,449	17,042	11,665	4,269	–3,546	–11,973	–20,699	–29,729

Table 13. NPV depends on the electricity rate and system size

DISCUSSION

A compact prototype of PV-battery module had been successfully created and installed in the faculty of engineering, CULS. Tests are conducted to prove the prototype's safety and hereby summarized

Under load, the temperature increases at a higher rate if the system must run directly from the battery. If the PV module works in parallel with the battery, then the temperature will increase at a lower rate.

With the lower current discharge rate (<30 A), we expected the heat sink would be able to dissipate most of the heat generated by the battery during the discharge process.

With the higher current discharge rate (>30 A), the battery bank will not be able to operate for more than 2 h. The heat generated by the battery is directly proportional to the discharge current (ZHAO, et al., 2018). Therefore, if our system must operate under a high current demand load, the temperature of the battery is expected to increase to no less than 3.09 °C and no more than 6 °C (in the 2× higher current discharge rate) more than ambient temperature.

From the correlation of battery temperature and ambient temperature after long-term observation, it was seen that when the ambient temperature is 54.2 °C, the battery temperature will reach its maximum allowable temperature of 70 °C. It is important to remember that during

this observation, the battery was discharged only during the night with a low discharge current. If considering the high current discharging test, we predict the possible maximum ambient temperature for the safe operation of the system is 48 °C.

CONCLUSION

For off-grid application, one PV-battery module could ensure a self-sufficiency ratio greater than 90% only for systems requiring an annual consumption of less than 0.1 MWh per year. Higher energy demands the probability of energy shortage increases.

The system operation is strongly affected by the peak load demand. The best case is when the difference between peak load and other times is small. High peak load occurring during winter time might lead to a low self-consumption ratio and self-sufficiency ratio. Using a pattern with some resting days for the battery to recharge will slightly increase the system utilization.

Large battery capacity will improve the system self-consumption ratio and self-sufficiency ratio. The most suitable size of the battery is from 0.5 to 1 kWh with 70% of usable capacity. When the battery capacity is lower than 0.5 kWh, the total points drop because load demand during the night is not satisfied. On the opposite side, if the battery capacity is larger than 1 kWh, then total points drop because of higher LCOE and system cost.

In terms of system utilization by total points and NPV, one PV-battery module should serve an annual load demand of 0.5 MWh per year with a self-sufficiency ratio 70%. If more modules are used than necessary, the total points will reduce and stable at about 200 because the self-sufficiency ratio is maximum but self-consumption ratio and grid parity ratio decrease with system size. Unlike the points, NPV is not reduced when the load demand increases because of the same amount of energy saving. Each module could provide maximum NPV about CZK 2400

after 20 years of operation. Four or more modules must be used to make the sufficiency ratio 90%, and the system could be feasible when the electricity rate increases from 4 CZK to 8 CZK.

Future work might focus on the system with DC/AC inverter to make this PV-battery module become more user-friendly.

PUBLICATION AND ACTIVITIES

ABROAD ACTIVITIES

- Lecturing and research during the exchange program on the University of HKBP Nommensen (Indonesia) – Erasmus; Feb – May 2017

CONFERENCES PROCEEDING

Dang, M.Q., Kouřím, P. Libra, M., Poulek, V.
Temperature changes of Photovoltaic cells parameters
16th International Workshop for Young Scientists "BioPhys Spring 2017"; Poland

Dang, M.Q.
Solar Energy Potential in Indonesia
58th International Conference of Young Scientists „ICYS 2017"; Czech Republic

Dang, M.Q., Kouřím, P. Libra, M., Poulek, V.
Thermal behavior of solar PV battery panel in outdoor condition
17th International Workshop for Young Scientists "BioPhys Spring 2018"; Slovakia

PUBLICATION ON SCOPUS INDEXED JOURNALS

Beránek, V.; Olšan, T.; Libra, M.; Poulek, V.; Sedláček, J.; Dang, M.-Q.; Tyukhov, I.I.
New Monitoring System for Photovoltaic Power Plants' Management
Energies 2018, 11, 2495. https://doi.org/10.3390/en11102495

Minh-Quan Dang , J. Šafránková, M. Libra, V. Poulek, P. Kouřím, J. Sedláček
Autonomous Photovoltaic System for Night-time Lighting in the Stable
Agronomy Research 2019, Accepted

REFERENCES

ACANSKI, Milos, POPOVIC-GERBER, Jelena and FERREIRA, Braham. 2010. Thermal modeling of the module integrated DC-DC converter for thin-film PV modules. *Proceedings of 14th International Power Electronics and Motion Control Conference EPE-PEMC 2010.* 2010, pp. 160-165.

AVANCIS. 2019. Datasheet Avancis Solar Module. [Online] 2019. https://www.avancis.de/en/products/powermaxr-40/.

BARRÉ, Anthony, et al. 2013. A review on lithium-ion battery ageing mechanisms and estimations for automotive applications. *Journal of Power Sources.* 2013, Vol. 241, 680-689.

BLACK, Marcie R. and REVER, William B. 2017. Black Silicon: There's more than meets the eye. *PV-Tech.* [Online] 2017. https://www.pv-tech.org/guest-blog/black-silicon-theres-more-than-meets-the-eye.

British Petroleum. 2017. *BP Statistical Review of World Energy 2017.* London : BP PLC, 2017.

BROWN, G.F. and WU, J. 2009. Third generation photovoltaics. *Laser & Photonics Review.* 2009, Vol. 3, 4, pp. 394-405.

CADEX. 2019. BU-205: Types of Lithium-ion. *Battery University.* [Online] 2019. https://batteryuniversity.com/learn/article/types_of_lithium_ion.

CHEN, Dinguo. 2001. Anti-reflection (AR) coatings made by sol-gel processes: A review. *Solar Energy Materials and Solar Cells.* 2001, Vol. 68, 3-4, pp. 313-336.

Diego, SAN. 2019. After electric cars, what more will it take for batteries to change the face of energy? [Online] 2019. https://www.economist.com/briefing/2017/08/12/after-electric-cars-what-more-will-it-take-for-batteries-to-change-the-face-of-energy.

DIOUF, Boucar and PODE, Ramchandra. 2015. Potential of lithium-ion batteries in renewable energy. *Renewable Energy.* 2015, Vol. 76, 375-380.

EINSTEIN, Albert. 1905. Über einen die Erzeugung und Verwandlung des Lichtes betreffenden heuristischen Gesichtspunkt (On a Heuristic Point of View about the Creation and Conversion of Light). *Annalen der Physik.* 1905, Vol. 17, pp. 132 - 148.

First-Solar. 2019. Datasheet First Solar Series 6™ Solar Module. *First Solar.* [Online] Febuary 2019. http://www.firstsolar.com/-/media/First-Solar/Technical-Documents/Series-6-Datasheets/Series-6-Datasheet.

GREEN, Martin A. 2001. Third generation photovoltaics: Ultra-high conversion efficiency at low cost. *Progress in Photovoltaics: Research and Applications.* 2001, Vol. 9, 2, pp. 123-135.

GUIFANG, Han, et al. 2017. Towards high efficiency thin film solar cells. *Progress in Materials Science.* 2017, Vol. 87, pp. 246-291.

GUILLEVIN, N., et al. 2012. High Efficiency n-Type Metal Wrap through Cells and Modules. *Energy Procedia.* 2012, Vol. 27, pp. 610-616.

HALL, Max. 2019. PERC cell efficiency records tumble. *PV magazine International.* [Online] January 2019. https://www.pv-magazine.com/2019/01/17/perc-cell-efficiency-records-tumble/.

HARRINGTON, Rebecca. 2017. This incredible fact should get you psyched about solar power — no matter what Trump does. *Bussiness Insider.* [Online] March 2017. https://www.businessinsider.com/solar-power-potential-how-much-energy-does-sun-have-2017-3.

Honsberg, Christiana and Bowden, Stuart. 2019. Terrestrial Solar Radiation. *PVeducation.* [Online] 2019. https://www.pveducation.org/pvcdrom/terrestrial-solar-radiation.

JAISWAL, Abhishek. 2017. Lithium-ion battery based renewable energy solution for off-grid electricity: A techno-economic analysis. *Renewable and Sustainable Energy Reviews.* 2017, Vol. 72, 922-934.

LIU, Jingjing, et al. 2018. Review of status developments of high-efficiency crystalline silicon solar cells. *Journal of Physics D: Applied Physics.* 2018, Vol. 51, 123001.

MASSON, Gaëtan, KAIZUKA, Izumi and BRUNISHOLZ, Mary. 2018. *A Snapshot of Global PV (1992-2017).* s.l. : Internation Energy Agency Photovoltaics Power Systems, 2018. ISBN 978-3-906042-72-5.

MERTENS, Konrad. 2014. *Photovoltaics Fundamentals, Technology and Practice.* s.l. : Wiley, 2014. ISBN 978-1118634165.

MOORTHI, Mumu. 2010. Lithium Titanate Based Batteries for High Rate and High Cycle Life Applications. [Online] 2010. https://neicorporation.com/white-papers/NEI_White_Paper_LTO.pdf.

NITTA, Naoki, et al. 2015. Li-ion battery materials: present and future. *Materials Today.* 2015, Vol. 18, 5, pp. 252-264.

OTE. 2018. Typové diagramy dodávek elektřiny. [Online] 2018. https://www.ote-cr.cz/en/statistics/electricity-load-profiles.

PETERS, Ian Marius and BUONASSISI, Tonio. 2018. Energy Yield Limits for Single-Junction Solar Cells. *Joule.* 2018, Vol. 2, 6, pp. 1160-1170.

PLANCK, Max. 1901. Ueber das Gesetz der Energieverteilung im Normalspectrum (On the Law of Distribution of Energy in the Normal Spectrum). *Annalen der Physik.* 1901, Vol. 4, pp. 202-237.

POULEK, Vladislav and LIBRA, Martin. 2010. *The Physical Principles of Photovoltaic Energy Conversion.* Prague : ILSA, 2010. ISBN 978-80-904311-2-6.

QCELLS. 2018. *Q CELLS Product Catalouge.* Germany : HANWHA Q CELLS GMBH, 2018. 2018-04_Rev01_EN.

REYNAUD, J.F., et al. 2008. Multifunctional module lithium-ion storage and photovoltaic conversion of solar energy. *2008 33rd IEEE Photovolatic Specialists Conference.* 2008.

ROTERS, G., et al. 2010. Heterojunction Technology: The Solar Cell of The Future. [Online] 2010. https://www.meyerburger.com/user_upload/dashboard_news_bundle/da4c7a0b7c33e8e21ccddace78c76513b12cc727.pdf.

SHOCKLEY, William and QUEISSER, Hans J. 1961. Detailed Balance Limit of Efficiency of p-n Junction Solar Cells. *Journal of Applied Physics.* 1961, Vol. 32, 3, pp. 510-519.

VEGA-GARITA, Victor, et al. 2016. Physical integration of PV-battery system: Advantages, challenges, and thermal model. *2016 IEEE International Energy Conference (ENERGYCON).* 2016.

WHITTINGHAM, M. S. 1976. Electrical Energy Storage and Intercalation Chemistry. *Science.* 1976, Vol. 192, 4244, pp. 1126-1127.

WILLS, R.H., et al. 1997. The AC photovoltaic module concept. *Proceedings of the Thirty-Second Intersociety Energy Conversion Engineering Conference.* 1997, No.97CH6203, pp. 1562-1563.

WOHLGEMUTH, John. 2012. IEC 61215: What It Is and Isn't (Presentation). *Conference presentation at the PV Module Reliability Workshop, 28 February - 2 March 2012, Golden, Colorado, USA.* 2012.

WÜRFEL, Peter and WÜRFEL, Uli. 2009. *Physics of solar cells: From basic principles to advanced concepts, second updated and expanded edition.* s.l. : Wiley, 2009. ISBN: 978-3-527-40857-3.

YAMAGUCHI, Masafumi, et al. 2018. A review of recent progress in heterogeneous silicon tandem solar cells. *Journal of Physics D: Applied Physics.* 2018, Vol. 51, 133002.

YOSHIKAWA, Kunta, et al. 2017. Silicon heterojunction solar cell with interdigitated back contacts for a photoconversion efficiency over 26%. *Nature Energy.* 2017, Vol. 2, 17032.

ZHAO, Chunrong, et al. 2018. Thermal behavior study of discharging/charging cylindrical lithium-ion battery module cooled by channeled liquid flow. *International Journal of Heat and Mass Transfer.* 2018, Vol. 120, pp. 751-762.

ZUBI, Ghassan, et al. 2018. The lithium-ion battery: State of the art and future perspectives. *Renewable and Sustainable Energy Reviews.* 2018, Vol. 89, pp. 292-308.